Michael D. Cahalan
K. George Chandy

The functional network of ion channels in T lymphocytes

Authors' address
Michael D. Cahalan[1], *K. George Chandy*[1]
[1]Department of Physiology and Biophysics, and the Institute for Immunology, University of California, Irvine, Irvine, CA, USA.

Correspondence to:
Michael D. Cahalan
285 Irvine Hall
University of California, Irvine
Irvine, CA 92697-4561, USA
Tel.: +1 949 824 7776
Fax: +1 949 824 3143
e-mail: mcahalan@uci.edu

Acknowledgements
The authors thank the many talented students, postdoctoral researchers, and collaborators who have participated in our 25-year journey of ion channel discovery in the immune system. Anna Amcheslavsky, Milton Greenberg, James Hall, Maria Lioudyno, Ian Parker, Heike Wulff, and Shenyuan Zhang contributed valuable comments during preparation of the manuscript, and Karinne Németh-Cahalan helped with figures. This work was supported by the NIH (NS-14609 and GM-41514 to MDC; and NS-048252 to KGC).

Immunological Reviews 2009
Vol. 231: 59–87

Immunological Reviews
0105-2896

Summary: For more than 25 years, it has been widely appreciated that Ca^{2+} influx is essential to trigger T-lymphocyte activation. Patch clamp analysis, molecular identification, and functional studies using blockers and genetic manipulation have shown that a unique contingent of ion channels orchestrates the initiation, intensity, and duration of the Ca^{2+} signal. Five distinct types of ion channels – Kv1.3, KCa3.1, Orai1+ stromal interacting molecule 1 (STIM1) [Ca^{2+}-release activating Ca^{2+} (CRAC) channel], TRPM7, and Cl_{swell} – comprise a network that performs functions vital for ongoing cellular homeostasis and for T-cell activation, offering potential targets for immunomodulation. Most recently, the roles of STIM1 and Orai1 have been revealed in triggering and forming the CRAC channel following T-cell receptor engagement. Kv1.3, KCa3.1, STIM1, and Orai1 have been found to cluster at the immunological synapse following contact with an antigen-presenting cell; we discuss how channels at the synapse might function to modulate local signaling. Immuno-imaging approaches are beginning to shed light on ion channel function *in vivo*. Importantly, the expression pattern of Ca^{2+} and K^+ channels and hence the functional network can adapt depending upon the state of differentiation and activation, and this allows for different stages of an immune response to be targeted specifically.

Keywords: *K^+ channel, CRAC channel, Ca^{2+} signaling, immunological synapse, autoimmune disorder, immunosuppression*

Introduction

Single cell assays, including electrophysiology and a variety of *in vitro* and *in vivo* imaging techniques, have offered unique insights into molecular and cellular mechanisms that underlie cellular activation. In particular, ion channels entered the immunological realm some 25 years ago when it became possible to record electrical signals from single cells of the immune system. In T cells, we have characterized five types of ionic currents, representing electrically the activity of distinct ion channels. Four of these have now been securely identified at the molecular level – most recently through the identification of stromal interacting molecule (STIM) and Orai proteins. Following T-cell receptor (TCR) engagement and endoplasmic reticulum (ER) Ca^{2+} store depletion, Ca^{2+} unbinds from STIM1's low-affinity luminal EF hand domain. This triggers STIM1 first to oligomerize and then to translocate (empty-

handed) to the plasma membrane where it activates Orai1 to form a Ca^{2+}-selective pore. Potent and selective channel blockers of the two types of K^+ channels, Kv1.3 and KCa3.1, have been identified and optimized, leading to a series of studies that showed their functional roles in Ca^{2+} signaling and lymphocyte activation.

It is now clear that ion channels form a functional network in lymphocytes at several levels. At the molecular level, STIM1 and Orai1 must come together to activate the CRAC channel following depletion of the ER Ca^{2+} store; and K^+ channels are physically associated with accessory subunits, forming potential links to integrin molecules, kinases, and the cytoskeleton. At the sub-cellular level, K^+ and Ca^{2+} channels accumulate at the immunological synapse with the potential to generate local ionic accumulation or depletion, to assemble molecular aggregates into signaling complexes, and to mediate trans-synaptic signaling. At the level of single cells, ion channels regulate global Ca^{2+} signaling that by an ionic balance of Ca^{2+} influx and K^+ efflux leads to changes in gene expression and motility; cell volume is regulated by an ionic balance of Cl^- efflux and K^+ efflux. As their expression can vary greatly during activation and differentiation, Ca^{2+} and K^+ channels participate in a positive feedback loop that sensitizes T cells to produce a larger Ca^{2+} signal upon re-encountering antigen. Finally, at the level of potential therapeutic benefit, efficacy in animal models points toward a selective immunosuppressive strategy to target Kv1.3 channels for chronic inflammatory and autoimmune disorders, while KCa3.1 and CRAC channel blockers may effectively target acute activation events.

In this review, we provide an overview of how lymphocyte ion channels work at the molecular and biophysical levels, how they interact functionally to regulate Ca^{2+} signaling, motility, and cell volume, and how the lymphocyte channel phenotype changes during activation and differentiation. We summarize results of Kv1.3 blockers in preclinical studies on animal models. In addition, we provide speculation on the functional consequences of ion channel localization at the immunological synapse and discuss how immuno-imaging approaches are beginning to reveal channel function *in vivo*.

Biophysical fingerprint and molecular identity of ion channels in T lymphocytes

The development of patch-clamp recording methods by Neher, Sakmann and colleagues (1) provided the means to investigate ion channels in lymphocytes, well before their molecular identities were revealed. Whole-cell recording in human T cells led to the definition of a unique biophysical fingerprint for each of five types of current, all having distinct channel activation requirements. Single-channel recording contributed to this fingerprint and also enabled the number of channels per cell to be determined with single-molecule precision. Ultimately, by comparing the biophysical properties with candidate genes expressed in heterologous systems, the molecular identities of K^+ and Ca^{2+} channels – two of each – were revealed. *Fig. 1* illustrates the five major types of ion channels that have been extensively studied in T lymphocytes.

Kv1.3 and voltage-gated K^+ current, K_V

We (2, 3) and others (4, 5) initially described a voltage-gated K^+ current in human and murine T cells. The K^+ current activates when the membrane potential is depolarized (more positive inside the cell), and as a result, K^+ ions move outward, passively leaving the cell down the K^+ electrochemical gradient. The process of channel opening is referred to as activation gating. A second gating property called inactivation closes the channel slowly if the membrane potential remains depolarized. Unlike the classical 'ball and chain' mechanism of inactivation described for many other K^+ channels, the lymphocyte channel inactivates by a conformational change at the external side of the channel pore (6–8), resulting in use-dependent or cumulative inactivation during repeated episodes of depolarization.

These channel-gating characteristics, along with single channel properties and a distinctive pharmacological profile described below, provided a unique biophysical fingerprint that enabled the lymphocyte K^+ channel to be identified as Kv1.3 (HUGO name KCNA3, formerly named MK3, RGK5, or HLK3) (9–11), one of approximately 80 distinct K^+ channel genes in the human genome. The Kv1.3 channel, like about half of all K^+ channels, is intrinsically voltage dependent; its conformation changes when the cell is depolarized, leading to an open channel that is specific to K^+ ions. The pore for specific conduction of K^+ ions is right in the middle of subunits pre-assembled as a tetramer. A single resting T cell obtained from human peripheral blood typically has approximately 400 functional Kv1.3 channels in the plasma membrane (2). In T cells under basal conditions, the resting potential is maintained at about −50 mV by only a small fraction of the available Kv1.3 channels (2, 12, 13). In essence, Kv1.3 by its sigmoid voltage dependence provides protection against depolarization of the membrane potential, thereby ensuring that the lymphocyte's membrane potential does not become significantly depolarized, even if Ca^{2+} is entering the cell (*Fig. 2A*).

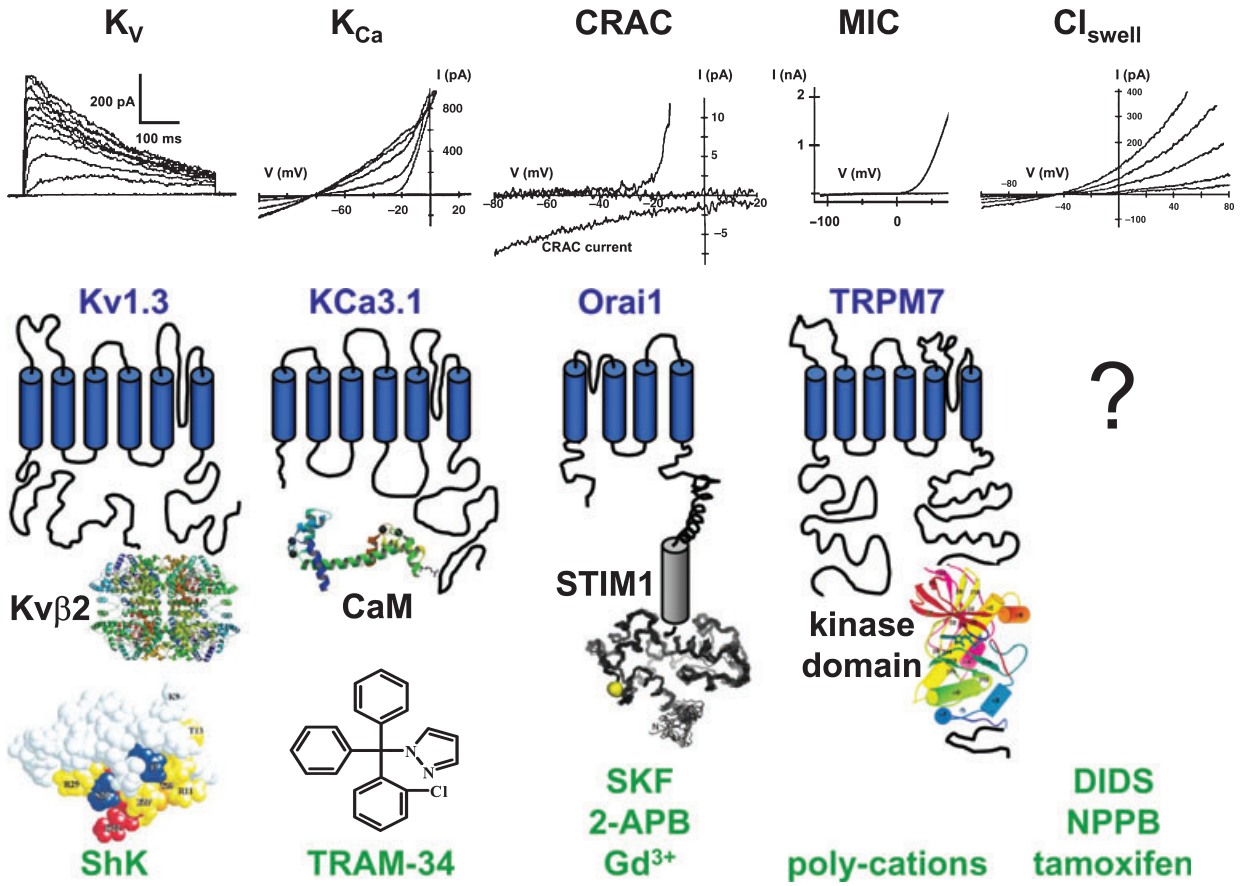

***Fig. 1.* Five types of ion channels in T lymphocytes.** From top to bottom: whole-cell current fingerprints (10, 50, 64, 111, 126); molecular identities of membrane-spanning subunits and accessory subunits or domains; and examples of channel blockers including ShK sea anemone peptide toxin (lower left) showing the critical lysine 22 in red (38). From left to right: voltage-gated K^+ channel (Kv1.3), with structure of Kvβ2 (227); Ca^{2+}-activated K^+ channel (KCa3.1), with CaM structure (PDB 1up5); CRAC channel (Orai1 + STIM1), EF-SAM domain structure of STIM1 (292); MIC channel (TRPM7), kinase domain structure (293); and Cl_{swell} of uncertain molecular composition. CRAC, Ca^{2+}-release activating Ca^{2+} channel; STIM, stromal interacting molecule; MIC, Mg^{2+}-inhibited Ca^{2+}-permeable current; Cl_{swell}, swelling-activated Cl^- channel; CaM, calmodulin.

Kv1.3 is found in the plasma membrane of T cells as part of a signaling complex that includes β1-integrin, a PDZ-domain protein called hDlg (or SAP97), an auxiliary channel subunit Kvβ2, an adapter protein ZIP (a.k.a. sequestosome 1/p62), and $p56^{lck}$ (Lck) (14, 15). It is also present in the inner membrane of mitochondria, where it has been reported to be the target for the apoptotic BAX protein, which binds and occludes the channel pore, thereby altering the membrane potential of the mitochondrion (16, 17).

Relative to other ion channels, Kv1.3 has an unusually broad sensitivity to pharmacological agents, including some that are usually thought of as hitting different molecular targets. As reviewed previously (14), Kv1.3 is blocked by small organic compounds in the millimolar to nanomolar range as well as peptide toxins in the nanomolar to picomolar range of potency. The portfolio of Kv1.3 blockers includes (in the approximate order of discovery) canonical but low potency agents previously known to block 'delayed rectifier' K^+ channels in nerve (2, 3, 18), ionic blockers (19), Ca^{2+} antagonists, and calmodulin (CaM) antagonists (18, 19), scorpion peptides (20–25), sea anemone peptides (26–28), compounds discovered as a result of high-throughput screening efforts (8, 29–31), progesterone (32), and non-peptidyl compounds resulting from a screen of compounds isolated from the shrub plant *Ruta graveolens* and the carrot family plant *Ammi visnaga* (33, 34). For the scorpion and sea anemone peptide toxins, alanine scanning and complementary mutagenesis have revealed the binding interactions with Kv1.3 (28, 35–39). These toxins block from the outside, like a cork in a bottle. A critical positively charged lysine residue on the toxin partially enters the pore between subunits of the tetrameric channel, occupying a site where K^+ ions normally bind. Several scorpion and sea anemone peptide toxin variants with improved selectivity for Kv1.3 have been engineered (20, 40, 41), including a fluorescent toxin analog that can be used in flow cytometry (42). The most potent of these peptides,

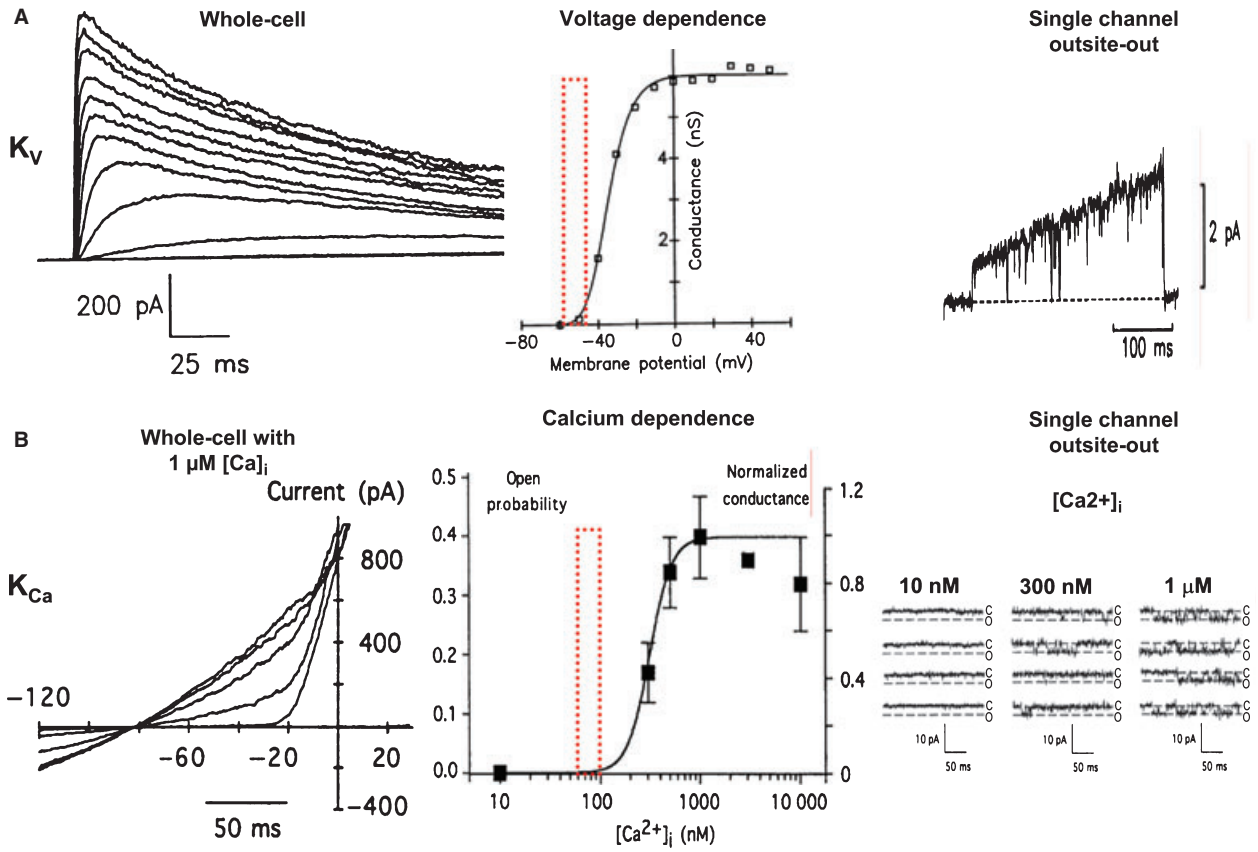

***Fig. 2.* Biophysical characteristics of K^+ channels in T lymphocytes.** (A) Voltage-gated K^+ current (from 22, 147). From left to right: whole-cell currents in response to step depolarization to varying potentials, voltage dependence of channel opening (red box shows normal range of resting membrane potential near the foot of the channel activation curve); outside-out patch single-channel current in response to a voltage ramp stimulus. (B) Ca^{2+}-activated K^+ current (from 50). From left to right: whole cell currents increasing as Ca^{2+} enters the cytosol; Ca^{2+} dependence of channel opening (red box shows normal range of cytosolic Ca^{2+} levels at rest, indicating lack of KCa3.1 channel activation until after the Ca^{2+} signal is initiated); single channels in inside-out patch exposed to varying Ca^{2+} concentrations.

OSK-1-Lys^{16}Asp^{20}, blocks with an IC_{50} value of 3 pM and exhibits >300-fold selectivity for Kv1.3 over closely related K^+ channels (41). The BmKTX-Arg^{11}Thr^{28}His^{33} peptide inhibitor (ADWX-1) was reported to block Kv1.3 with an IC_{50} value of 1 pM (20), but we found this peptide to have 1000-fold lower potency (IC_{50} 1.2 nM, K.G. Chandy, unpublished data). A variety of small organic inhibitors block Kv1.3 by gaining access to the inner vestibule of the channel (29, 43–48), and several of these lipophilic compounds stabilize the inactivated state of the channel. The most potent non-peptidyl inhibitor of Kv1.3 is PAP-1 with an IC_{50} value of 2 nM (49).

KCa3.1 and Ca^{2+}-activated K^+ current, K_{Ca}

A second type of K^+ current in T cells is activated by a rise in cytosolic Ca^{2+}, rather than by changes in membrane potential (*Fig.* 2B). In human T and B cells (but not in Jurkat cells), the Ca^{2+}-activated K^+ current is characterized by an intermediate single channel conductance that uniquely distinguishes it from small- or large-conductance Ca^{2+}-activated K^+ channels (50). The channel is closed under resting conditions with low basal cytosolic Ca^{2+} and opens rapidly if Ca^{2+} rises, with an effective binding coefficient of approximately 300 nM and a high degree of cooperativity consistent with a tetrameric channel. The essential pore-forming subunit is KCa3.1 (HUGO name KCNN4, formerly named IKCa1 or SK4) (51–53), with a six-transmembrane segment architecture and a tetrameric pore similar to Kv1.3 and other voltage-gated K^+ channels. CaM bound to the C-terminus of the KCa3.1 subunit functions as an essential Ca^{2+}-sensing subunit to activate the channel rapidly upon Ca^{2+} binding (54). Thus, during TCR-evoked Ca^{2+} signaling, the opening of KCa3.1 channels contributes a K^+ current that makes the membrane potential more negative (hyperpolarized). In $CD4^+$ T cells, K_{Ca}3.1 activity is increased by the nucleoside diphosphate kinase B (NDPK-B), which phosphorylates K_{Ca}3.1 on histidine 358, and by phosphatidylinositol-3 phosphatase (55, 56). Interestingly,

histidine 358 is dephosphorylated by the mammalian protein histidine phosphatase (PHPT-1), which directly binds to the $K_{Ca}3.1$ protein and negatively regulates T-cell Ca^{2+} flux and proliferation by decreasing $K_{Ca}3.1$ activity (56). If PHPT-1 is knocked out, T cells have a bigger calcium signal and proliferate more vigorously. $K_{Ca}3.1$ modulation in T cells is thus one of the rare examples of histidine phosphorylation/dephosphorylation influencing biological processes in mammals. Functional activation of KCa3.1 by phosphatidylinositol-3 phosphatase is opposed by the PI(3)P phosphatase myotubularin-related protein 6, which suppresses calcium signaling and cell proliferation (57, 58).

A variety of non-peptidyl compounds and peptides inhibit KCa3.1 channels. These include clotrimazole and two more potent and selective analogs TRAM-34 (53, 59–61) and ICA-17043 (62), charybdotoxin (50) and its analog ChTX-E32 (37), ShK (38), and maurotoxin (63).

STIM1 and Orai1, CRAC current

After many different approaches were explored, perforated patch recording combined with cytosolic Ca^{2+} monitoring revealed a tiny inward Ca^{2+} current in Jurkat T cells that corresponded closely to the rise in cytosolic Ca^{2+} concentration evoked by TCR stimulation with PHA (64). In the perforated patch recording configuration, the membrane beneath the pipette is permeabilized by a pore-forming antibiotic to allow electrical access between the pipette and cytoplasm but without dialyzing the cell. Thus, signal transduction pathways within the cell are preserved during electrical recording and stimulation. Varying the membrane potential and ionic conditions revealed a unique biophysical fingerprint of a low-conductance, inwardly rectifying, Ca^{2+}-selective current that is blocked by Ni^{2+} ions (64). As T lymphocytes are small and have resting Ca^{2+} concentration of approximately 50 nM, corresponding to fewer than 10 000 free Ca^{2+} ions, a tiny Ca^{2+}-selective current of only a few picoamperes is capable of producing a substantial rise in cytosolic Ca^{2+} concentration. A biophysically indistinguishable Ca^{2+}-selective current in T cells and mast cells is evoked by several stimuli – all of which deplete the intracellular store of Ca^{2+} in the ER – including TCR engagement, addition of a Ca^{2+} ionophore such as ionomycin, addition of IP_3 or a Ca^{2+} chelator by dialysis from the patch pipette into the cytoplasm, and by thapsigargin, a specific inhibitor of the SERCA (sarco/enodoplasmic reticulum Ca^{2+} adenosine triphosphatases, ATPase) pump in the ER membrane (65–67). Hence, the current was named Ca^{2+} release-activated Ca^{2+} (CRAC) current. The common denominator of these activating stimuli is depletion of ER luminal Ca^{2+} *per se*, rather than the resulting rise in cytosolic Ca^{2+}. The lymphocyte CRAC current is a highly Ca^{2+}-selective type of 'store-operated' Ca^{2+} entry channel (permeability ratios >1000 for Ca^{2+} over monovalent cations). More than 15 years passed by from the first detection of CRAC current to the identification of molecules that underlie it. *Fig. 3A* illustrates Kv1.3 and CRAC current in a Jurkat T cell.

Although physiologically the CRAC channel is triggered in lymphocytes and mast cells by IP_3-induced depletion of the ER Ca^{2+} store, the key breakthrough in defining the molecules came from RNA interference (RNAi) screening performed in other cell types to search for genes that are essential for thapsigargin-induced Ca^{2+} influx. Thapsigargin irreversibly blocks the SERCA pump in the ER membrane and activates CRAC current by depleting the luminal store of Ca^{2+} through passive leak of Ca^{2+} from the ER into cytoplasm unopposed by active reuptake. Thapsigargin activates CRAC current while bypassing the entire proximal signal transduction cascade leading from receptor engagement. *Drosophila* S2 cells were used in a candidate screen that identified *Stim* as the only gene among 170 tested that was essential for normal thapsigargin-evoked Ca^{2+} influx (68). S2 cells are ideal for RNAi screening because they spontaneously take up double-stranded RNA that is then processed by an intracellular ribonuclease, Dicer, to generate short interfering RNA (siRNA) species that break down messenger RNA (mRNA) selectively inside the cell. As luck would have it, our patch-clamp analysis of S2 cells demonstrated a *bona fide* CRAC current with all of the biophysical characteristics of CRAC current in human T cells (69), providing confidence that the RNAi screening approach in S2 cells would successfully reveal a molecular mechanism shared by human immune cells. We showed that *Drosophila* Stim and the human homolog STIM1 are essential for CRAC current in S2 cells and Jurkat T cells, respectively (68). An independently conducted screen of HeLa cells using a Diced library of about 2000 genes identified both human homologs, STIM1 and STIM2 (70).

Years before it came to light in the Ca^{2+} signaling field, STIM1 was identified in a functional screen to detect surface molecules required for binding of pre-B cells to stromal cells and given the name SIM (71), which later morphed into STIM. This functional identification implies that plasma membrane-resident STIM1, estimated at 20–30% of the cell's total content of STIM1 by surface biotinylation (72), may perform a cell adhesion function. We can now regard the naming of Stim proteins as completely appropriate to the functional role of ER-resident Stim in STIM-ulating store-operated Ca^{2+} influx. When the ER Ca^{2+} store is depleted, Stim proteins

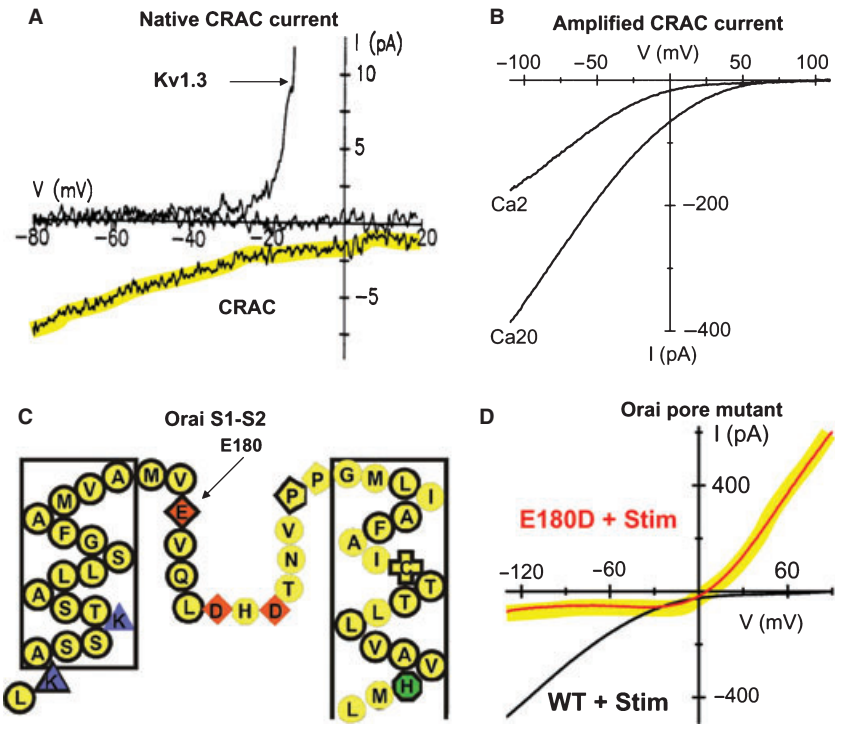

***Fig. 3.* CRAC channel.** (A) Native CRAC current (yellow highlighted trace) in Jurkat T cells activated during passive store depletion (from 64). (B) Amplified CRAC current in S2 cells co-transfected with Stim + Orai (from 78). Note the difference in current scales and the increase in current size when the extracellular Ca^{2+} concentration is increased from 2 to 20 mM. Amplified CRAC currents represent approximately 10^5 channels per cell or 100 functional channels per μm^2 of membrane surface in the overexpression system. (C) Orai sequence from first to second transmembrane segments. Residues conserved in Orai, Orai1, Orai2, and Orai3 are shown in bold. E180 Orai corresponds to E106 in Orai1. (D) Altered ion selectivity resulting from a conservative point mutation of Orai from glutamate to aspartate at position 180. Point mutation of this critical glutamate converts CRAC current from inwardly rectifying and Ca^{2+} selective to outwardly rectifying and monovalent cation selective (yellow highlighted trace). Stim was co-expressed to amplify CRAC currents (recordings from 87). CRAC, Ca^{2+}-release activating Ca^{2+} channel; Stim, stromal interacting molecule.

physically convey the signal from the ER to the plasma membrane to activate CRAC channels (70, 73, reviewed in 74). The N-terminus of Stim residing within the ER lumen contains a low-affinity EF-hand domain that binds Ca^{2+} when the Ca^{2+} store is filled. If the ER store is depleted, Ca^{2+} ions unbind from Stim, and Stim proteins migrate toward and accumulate in puncta next to the plasma membrane. Once it is immediately adjacent to the plasma membrane, i.e. within 10–25 nm observed using electron microscopy (75), Stim triggers CRAC channels formed by Orai subunits to open, allowing Ca^{2+} to enter the cell. In lymphocytes this entire process takes place within a minute following TCR engagement.

Three subsequent genome-wide screens again used thapsigargin in S2 cells, one that tracked nuclear factor of activated T cells (NFAT) translocation to the nucleus and two that monitored Ca^{2+} signaling, to identify additional required genes, including *Drosophila* Orai (CRACM) (76–78), a gene with three human homologs: Orai1, Orai2, and Orai3 (HUGO names ORAI1, ORAI2, and ORAI3). Of particular significance, homozygous expression of Orai1 bearing a point mutation (R91W) results in a nearly complete loss of store-operated Ca^{2+} entry and CRAC channel function in T-cell lines from patients with a rare recessive familial form of severe combined immune deficiency (SCID) (76), as described by Feske in this volume. Previous reports had shown that CRAC channels were non-functional in some human SCID patients (79–81), and additional mutations in STIM1 and Orai1 from such patients have recently been described (S. Feske, personal communication and 82). Consistent with a requirement for both Stim and Orai working together and showing that other cellular components are not limiting for functional expression, co-expression of Stim + Orai (or STIM1 + Orai1) yielded greatly amplified CRAC current amplitudes with normal biophysical characteristics (78, 83, 84) (*Fig. 3B*). Finally, clinching the identification of Orai (Orai1) as the pore-forming subunit of the CRAC channel, three groups independently showed that mutation of a conserved glutamate residue to aspartate produced a dramatic alteration in ion selectivity such that the CRAC channel activated normally but conducted monovalent cations instead of being selective for Ca^{2+} (85–87) (*Fig. 3C,D*). Orai2 and Orai3 are also capable of forming a CRAC-like current when expressed together with STIM1 in heterologous

cells (84, 88, 89). Collectively, these studies demonstrated that Stim and Orai proteins are both required for CRAC channel function in *Drosophila* and humans, that Stim initiates the process by sensing ER Ca^{2+} depletion and conveying the message to the plasma membrane, and that Orai forms the conducting pore of the CRAC channel. In T cells, CRAC channels triggered by STIM1 and formed by Orai1 are required for Ca^{2+} entry, based upon RNA knockdown of STIM1 and Orai1 in human T-cell lines (68, 76, 90) and in human T cells (91), and from nearly complete inhibition of thapsigargin- or TCR-induced Ca^{2+} entry by dominant-negative constructs of Orai1 in human T cells (90, 91). Analysis of knockout mice is presented elsewhere in this volume.

The discoveries of Stim and Orai opened the floodgates for recent investigation into the molecular mechanism of CRAC channel activation and the physiological roles of Stim and Orai homologs in various cell types. By co-immunoprecipitation (87), nanometer-scale fluorescence resonance energy transfer (FRET) imaging (92–95), and most recently by biochemical analysis of binding by the purified proteins *in vitro* (96), the molecular interaction between STIM1 and Orai1 is convincingly shown to be a direct binding interaction. As described above, Ca^{2+} sensing and signal initiation are mediated by the N-terminus of Stim within the ER lumen in sequential steps of oligomerization followed by translocation to the plasma membrane (94, 97, 98). The effector domain of Stim and STIM1 resides within the C-terminal end of the protein situated in the cytosol (94, 99–103). Expression of the C-terminus as a cytosolic protein effectively activates CRAC current through the Orai1 (or Orai) channel (94, 99–103), as do fragments of the C-terminus as small as 100 amino acids corresponding to the distal coiled-coil domain (96, 104, 105). Not only does STIM1 translocate to the ER–plasma membrane to activate Orai1 channels, it also organizes them into mirror clusters in the PM (106, 107), thereby augmenting local Ca^{2+} influx. Stim also appears to play a role in determining the stoichiometry of Orai subunits. Orai1 forms relatively stable dimers in cells (90, 101), but functional data from tandem tetramers of Orai1 strongly suggested that Orai1 is a tetramer when it forms a CRAC channel (108). Potentially reconciling these studies, when expressed alone, Orai was seen by single-molecule photobleaching as a dimer, but when expressed as a conducting channel activated by the C-terminus of Stim, Orai was shown to be tetrameric (101). These results suggest that Stim coordinates assembly of stable but inactive Orai dimers into functional tetramers. Clustering of STIM1 and Orai1 in T cells may have particular functional importance to amplify local Ca^{2+} signals at the immunological synapse (91) (see the Channels at the immunological synapse section).

Swelling-activated Cl^- current, Cl_{swell}: role in cell volume regulation

During our initial experimental phase of attempting to record Ca^{2+} current in T cells, we noticed that addition of ATP to the pipette (making the solution hypertonic) promoted activation of a novel outwardly rectifying chloride current (22), leading to the first electrophysiological characterization of an anion and osmolyte efflux that is activated by cell swelling in many cell types (109). This current has been termed Cl_{swell} or volume-regulated anion current (VRAC). In our first observations, the pipette solution containing ATP was inadvertently hypertonic and caused the cell to swell as we recorded, resulting in the activation of Cl^- current (22). Moreover, the same current could be activated reversibly by exposure to hypotonic extracellular solution (110, 111). Cl^- current is induced with a delay of about 1 min following cell swelling, and sustained current is dependent upon cytosolic ATP (111). Interestingly, hypotonic activation of Cl_{swell} was found to be defective in Lck-deficient T cells, and re-expression of Lck restored osmotic anion current activation (112). In this study, cell swelling was also shown to activate Lck kinase activity transiently to autophosphorylate. Thus, a phosphorylation event, consistent with the requirement for ATP, may be required to activate the Cl^- channel following cell swelling. In addition to Cl^- ions, the channel also conducts anions such as iodide, bromide, and nitrate, and has a lower permeability to amino acids such as aspartate and glutamate (111).

The molecular identity of swelling-activated Cl^- channels remains enigmatic. Among previously proposed candidate genes, swelling-activated Cl^- conductance is not due to P-glycoprotein, i.e. the multi-drug resistance gene (113), and is very unlikely to be a ClC family member (114). The most likely candidates at present are homologs of bestrophin (115) or TMEM16A (anoctamin) (116), but both have been associated with a Ca^{2+}-activated Cl^- channel with different biophysical properties.

Cl_{swell} and Kv1.3 work together functionally in T cells in the regulation of cellular volume (22, 117, 118). In response to cell swelling, the activation of Cl^- current triggers regulatory volume decrease (RVD) (22, 118). In mature T cells, RVD is Ca^{2+} independent. Cell swelling activates the chloride conductance and, as a result, the membrane potential depolarizes toward the chloride equilibrium potential of −35 mV due to negatively charged Cl^- ions leaving the cell. The resultant depolarization in turn activates Kv1.3 channels. Consequently,

the membrane potential remains in between the resting potential and the chloride equilibrium potential, and the cell loses both K^+ and Cl^-. After several minutes, during which water molecules are also lost, the cell shrinks back to the original volume and the chloride channel shuts. Consistent with Kv1.3 being the main efflux pathway in T cells, the ability to undergo RVD parallels the level of expression of voltage-gated K^+ conductance, and RVD is inhibited by K^+ channel blockers (119). In thymocytes, RVD has a Ca^{2+}-dependent component that is independent of CRAC channel activity; it is triggered by a stretch-activated Ca^{2+} influx that leads to activation of Ca^{2+}-activated K^+ current (118). Thus, KCa3.1 channels are recruited to promote RVD in thymocytes. The combined efflux of K^+ ions through both Kv1.3 and KCa3.1 restores the cell volume more rapidly than either one alone (118). Physiologically, RVD may come into play homeostatically for ongoing adjustment of T-cell volume and intracellular tonicity and to restore normal volume in response to a diluting environment within the kidney.

TRPM7 and MIC current, role in Mg^{2+} homeostasis

Years after K_V, K_{Ca}, Cl_{swell}, and CRAC currents were described, yet another current was characterized in T cells, specifically when Mg^{2+} ions were omitted from the pipette solution (120). This current exhibited outward rectification and carried monovalent and divalent cations non-specifically. Now referred to as the Mg^{2+}-inhibited Ca^{2+}-permeable (MIC) current (121) and also termed MagNuM (for magnesium nucleotide metal) cation current (122), the current develops with a similar time course to CRAC current during whole-cell recording but exhibits distinct biophysical properties. It has a much larger single-channel conductance, a different mechanism of activation, much less ion selectivity among cations, and different pharmacological sensitivities (121–123). MIC current is found in resting and activated T cells, in thymocytes, and in numerous other cell types (124–130).

The cloning of TRPM7 (originally named LTRPC7 or TRPPLIK) and studies on heterologous cell types clarified the molecular identity of the outward-rectifying MIC (MagNuM) current, and raised new issues of the channel-gating mechanism (131, 132). The protein consists of a typical TRP channel domain that presumably forms a tetrameric pore through which both monovalent and divalent cations can pass, followed by a long C-terminal tail that includes a functional α kinase domain. Conducting transmembrane current and having intrinsic kinase activity, this is one of the few channel-enzymes that exist. At the molecular level, the mechanism by which cytosolic Mg^{2+} inhibits MIC–TRPM7 current has been controversial. As Mg^{2+}-ATP binds to the cytosolic kinase domain, it was natural to investigate whether kinase activity is essential for channel activity. This approach led to discrepant results. One group (133, 134) reported altered channel activity by kinase-disrupting mutations. However, in our hands, mutation of the kinase binding site for Mg^{2+}-ATP to disrupt kinase activity did not affect MIC channel activity or sensitivity to inhibition by cytosolic Mg^{2+} (135). In our view, a more likely mechanism for channel inhibition by intracellular Mg^{2+} ions is by charge screening in which the negative charge of phosphatidylinositol 4,5-bisphosphate (PIP_2) is effectively screened by Mg^{2+} (or other) divalent cations (126, 136), consistent with the proposal from Clapham's group (137). PIP2, the membrane lipid that is cleaved to generate IP_3, associates with TRPM7 when Mg^{2+} is depleted and triggers channel activity. A similar PIP2-channel interaction requirement is found in several other channel types (138).

As the MIC–TRPM7 channel is permeable to Mg^{2+} ions (a very unusual channel characteristic) and can be opened by depletion of Mg^{2+} from the cytosol, a role in cellular Mg^{2+} homeostasis was suggested and tested in chicken DT-40 B cells (139). In the proposed homeostatic mechanism, if cytosolic Mg^{2+} levels fall, channel activity increases allowing Mg^{2+} to enter the cell to replenish cytosolic Mg^{2+}. Consistent with this hypothesis, disruption of the *Trpm7* gene resulted in a requirement for very high concentrations of extracellular Mg^{2+} for survival (139). Again consistent with a role in whole-body Mg^{2+} homeostasis, a similar TRP channel kinase, TRPM6, forms heteromultimers with TRPM7 and mutations in TRPM6 that disrupt the interaction with TRPM7 cause hypomagnesemia (140). However, directly contradicting the Mg^{2+} homeostasis hypothesis as it relates to resting T cells, genetic deletion of TRPM7 in the T-cell lineage specifically ablated MIC current in freshly isolated T cells but did not alter Mg^{2+} homeostasis of T cells exposed to varying extracellular Mg^{2+} levels (125). This study indicates that TRPM7–MIC current is not the primary cellular pathway for Mg^{2+} flux across the plasma membrane in resting T cells. It was also shown that genetic deletion of TRPM7 results in embryonic lethality, indicating a required role during early development (125). Moreover, thymic development was abnormal in Lck-CRE mice lacking TRPM7 in mature thymocytes and T cells, and there was a reduction in the total number of mature T cells and a higher percentage of $CD4^-CD8^-$ (double negative, DN) thymocytes, suggestive of a partial block in the transition from DN to double positive $CD4^+CD8^+$ thymocytes. With regard to Mg^{2+} homeostasis, however, a different study showed that TRPM7-

deficient lymphocytes were unable to proliferate in normal media but proliferated normally in media supplemented with Mg^{2+} (141). One way to reconcile these results on activated T cells with those from Jin *et al.* (125) is to postulate a requirement for TRPM7 in Mg^{2+} homeostasis only when T cells are activated or proliferating, and there is evidence that TRPM7 levels are upregulated in acutely activated T-cell blasts (124). A possible functional role of MIC–TRPM7 in the immune response remains uncertain; additional functions of TRPM7 related to cell volume regulation (142) and to release of synaptic vesicles (143, 144) have been proposed in other cell types.

Other channel types

In addition to the five main channel types found in T lymphocytes profiled above, other channel activities have been reported. A very small fraction (1–5%) of normal human T cells express detectable voltage-gated Na^+ current (2), even though these cells are not thought of as being electrically excitable. Additional types of K^+ current have been observed. For example, in mouse T cells, a second type of voltage-gated K^+ current with properties distinct from Kv1.3 is found in DN and $CD8^+$ T cells from the thymus and particularly in DN T cells from MRL/MpJ-lpr/lpr mice (145–150). This current results from Kv3.1 (151), but it has not been seen in human T cells. In addition to Kv1.3 and Kv3.1, other voltage-gated K^+ channels including Kv1.1, Kv1.2, and Kv1.6 have been reported in mouse T cells (152, 153) but not in human T cells. A two-pore TRESK-related K^+ channel that is not voltage dependent has also been described in Jurkat T cells (154) and TASK1 and TASK3 have been reported in human T cells (155). However, in our studies on 'normal' primary human T cells, all of the potassium current can be inhibited by the combination of ShK-Dap^{22} (selective Kv1.3 blocker) and TRAM-34 (selective KCa3.1 blocker), suggesting that Kv1.3 and KCa3.1 are the two main K^+ channels in human T cells. The human Jurkat T-cell line exhibits unusual expression of a small-conductance Ca^{2+}-activated K^+ current (156) produced by KCa2.2 (157), and of a Ca^{2+}-activated non-selective cation current due to TRPM4 (158). To our knowledge, these currents have not been observed in human T cells. Jurkat T cells and monocyte cell lines also reportedly express cyclic ADP ribose-activated channel activity (159–161) or Ca^{2+} influx (162) that may be due to TRPM2 (LTRPC2), but again these have not been reported in primary human T cells. It has been difficult to establish whether any TRP channels other than TRPM7 are expressed functionally in T cells (163). Once among the leading candidates to underlie CRAC current, several TRPC and TRPV family members are indeed detected in T cells by reverse transcriptase polymerase chain reaction (RT-PCR) (164), but studies of protein expression and functional channel activity are lacking. Among TRP-family channels, only outwardly rectifying TRPM7 cation currents are consistently observed in primary T cells (124, 126).

Perhaps the channel type that has attracted the most controversy regarding functional expression is the voltage-gated Ca^{2+} channel. During the first exploratory phase of patch clamp experimentation, we tried to detect Ca^{2+} ion movement across the cell membrane, initially without success (2, 3). In cardiac and other excitable cell types expressing CaV α subunits, membrane depolarization evokes Ca^{2+} current that is readily detected, and we adopted protocols designed to detect voltage-gated Ca^{2+} current, using Cs^+ to replace K^+ in the pipette. Instead of revealing Ca^{2+} current, whole-cell recording revealed only inward K^+ current as external K^+ ions moved inward through voltage-gated K^+ channels, essentially masquerading as an inward current channel. Ca^{2+} imaging, perhaps an even more sensitive way to detect functional activity of voltage-gated Ca^{2+} channels, also failed to detect voltage-dependent Ca^{2+} influx evoked by membrane depolarization. Instead, membrane depolarization inhibits Ca^{2+} influx (165), and K^+- or toxin-induced depolarization inhibits lymphocyte activation (166, 167). Furthermore, reports that Ca^{2+} antagonists, known to block cardiac L-type voltage-gated Ca^{2+} current, inhibit various T-cell functions are confounded by the fact that such antagonists in fact block voltage-gated K^+ current through Kv1.3 channels, with low micromolar potency (14, 18, 19). Nifedipine also blocks KCa3.1 channels (59). Whereas biochemical evidence of expression of various α-subunits of L-type Ca^{2+} channels has been reported in T and B lymphocytes (168–175), evidence for functional voltage-gated Ca^{2+} channels, i.e. those through which Ca^{2+} ions enter T cells, is lacking. Although CaV α-subunits were present in SCID patient T cells lacking CRAC current, these cells exhibited no Ca^{2+} current in response to membrane depolarization either before or after TCR stimulation (176). A recent re-examination of this question in resting and activated human T cells, using patch-clamp recording to test for voltage-gated Ca^{2+} channel activity and Ca^{2+} imaging to test for a Ca^{2+} signal evoked by K^+ depolarization, again turned up no evidence for voltage-gated Ca^{2+} channel activity (91). Moreover, voltage-gated Ca^{2+} channels, even if they are expressed, are unlikely to contribute to TCR-induced Ca^{2+} signaling, as SCID patient T cells bearing the Orai1 R91W mutation (76, 176) and Orai1 knockout T cells are

substantially impaired in TCR-induced Ca^{2+} influx (177). Finally, in both resting and activated human T cells, the expression of a dominant-negative point mutant of Orai1 with alanine replacing glutamate at the critical 106 position, completely inhibited Ca^{2+} influx due to TCR engagement and to thapsigargin (91). These studies demonstrate that the predominant Ca^{2+} influx pathway in human and mouse T cells is the CRAC channel formed from Orai1 subunits. Further work, including electrophysiological analysis, is needed on T-cell subsets that express CaV α-subunits to test for functional expression of voltage-gated Ca^{2+} channels. Might voltage sensors of CaV α-subunits exhibit other functions? In skeletal and cardiac muscle, CaV α-subunits not only mediate Ca^{2+} influx but also link directly to ryanodine receptors in the sarcoplasmic reticulum. Depolarization of the transverse tubular membrane, an invagination of plasma membrane, causes Ca^{2+} release from the SR via conformational changes in the CaV α-subunit voltage sensors. We return to this possibility below, in considering functions of ion channels localized to the immunological synapse.

Ca^{2+} signaling, T-cell motility, and gene expression

Ca^{2+} signaling in T cells came into its own following development by Roger Tsien and colleagues (178, 179) of the ratiometric Ca^{2+} indicator fura-2, allowing imaging of calibrated Ca^{2+} concentration within individual cells. A wide variety of cytosolic Ca^{2+} signals triggered by cross-linking of cell surface receptors have been reported, including sinusoidal sustained Ca^{2+} oscillations with a regular period of 1–2 min in Jurkat T cells (64), and Ca^{2+} transients, damped oscillations, or sustained oscillations in resting and acutely activated human T cells (165, 180). *Fig.* 4 illustrates an unabashedly channel-centric view of the signaling cascade from TCR engagement through NFAT promoter activity in the nucleus. Proximal signaling events leading to generation of IP_3 cause release of Ca^{2+} from the ER Ca^{2+} store. This component of the cytosolic Ca^{2+} signal due to Ca^{2+} released through ER IP_3 receptor channels is small – only about 100–200 nM – and insufficient to drive gene expression. ER Ca^{2+} store depletion triggers STIM1 to migrate to the plasma membrane and to activate Ca^{2+} influx through CRAC channels formed from Orai1 subunits. Ca^{2+} influx sends cytosolic Ca^{2+} concentration from a resting value of 50–100 nM into the low micromolar range of concentration. To sustain Ca^{2+} influx, a counterbalancing efflux of K^+ ions is needed, either through Kv1.3 or KCa3.1 or both. By its sigmoid voltage dependence, Kv1.3 prevents the cell from depolarizing even when CRAC channels open and enables the influx of Ca^{2+} to be sustained. In a local positive feedback loop, the rise in cytosolic Ca^{2+} activates KCa3.1, hyperpolarizes the membrane potential, and thus promotes further Ca^{2+} influx through the CRAC channel. The relative contribution of the two K^+ channels varies according to their relative expression level which changes during acute and chronic activation. During Ca^{2+} oscillations CRAC and Ca^{2+}-activated K^+ channels open and close in a regular sequence. CRAC channel activation leads the rise in intracellular Ca^{2+} concentration, but it inactivates before the peak of the Ca^{2+} signal (64), whereas Ca^{2+}-activated K^+ current activates at Ca^{2+} concentrations greater than approximately 200 nM and serve to sustain Ca^{2+} influx (181).

Cytosolic Ca^{2+} has also been monitored in T cells during antigen presentation *in vitro* (182–184) and in the native tissue environment (185–187). Motile polarized T cells naturally use their leading edge to come into contact with antigen-presenting cell (APC), as seen in the lymph node when T cells encounter dendritic cells (188). Indeed, T cells are most sensitive to TCR engagement at their leading edge (184, 189). Within 10 s of contact between the T cell and an APC, a Ca^{2+} signal is initiated that is uniform throughout the T cell, followed by a rapid increase in the area of close contact and T cell rounding up adjacent to the APC. Using thapsigargin and ionic gradients to vary cytosolic Ca^{2+} levels, the Ca^{2+} dependence of motility was determined (184). The 'STOP signal' produced by Ca^{2+} elevation alone is not transmitted by the NFAT pathway. Ca^{2+}-induced T-cell arrest is cyclosporine-insensitive; and it occurs much more rapidly (within a few minutes) than changes in gene expression, is rapidly reversible, and requires a lower degree of cytosolic Ca^{2+} elevation ($K_{effective}$ of approximately 300 nM). It may play a role in anchoring T cells to APCs, as increased buffering of cytosolic Ca^{2+} inhibited T-cell rounding and stable formation of T cell–APC conjugates (183, 184). Two studies monitored Ca^{2+} signals and motility during contact with dendritic cells in the lymph node environment (186, 187). Spiky Ca^{2+} signals are emitted that correlated with cell arrest on DCs. In thymocytes, Ca^{2+} signaling has been shown to be both necessary and sufficient for T-cell arrest on stromal cells during positive selection (185). Possible mechanisms and roles of Ca^{2+} and of integrins in producing STOP signals are discussed elsewhere (190, 191).

Critical to the outcome of the T cell–APC encounter, a T-cell Ca^{2+} signal must be of sufficient intensity and duration to result in changes in gene expression. The Ca^{2+} dependence and kinetics of NFAT-mediated gene expression were determined at the level of single cells using a gene expression

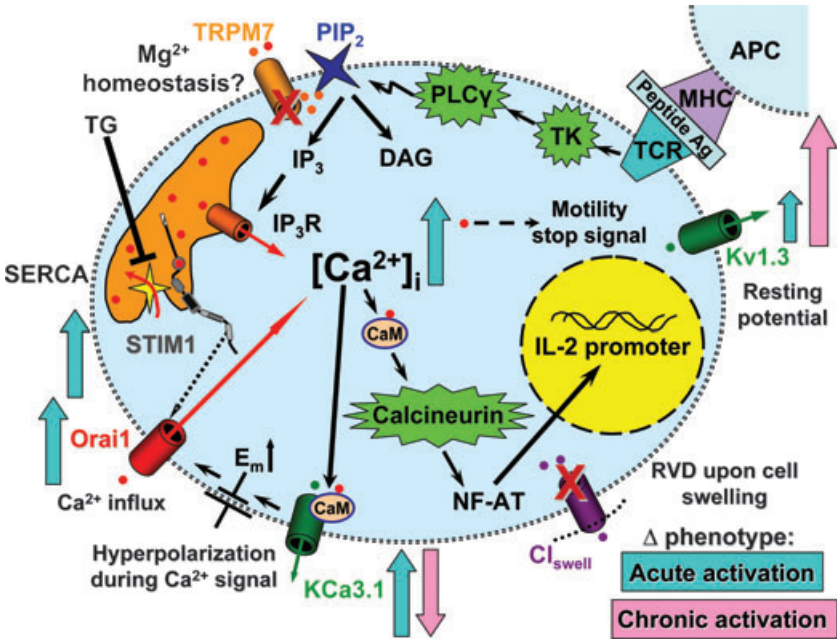

***Fig. 4.* Ion channels and Ca^{2+} signaling in T cells.** Signaling pathway from TCR engagement to gene expression in nucleus. Major ion channel types are color coordinated according to ion selectivity, Orai1 (red), Kv1.3 and KCa3.1 (green), cation non-selective TRPM7 and IP_3R channels (orange), and Cl_{swell} (violet). Dots and arrows correspond to ions and fluxes with the same color code. STIM1 is shown (gray) with a Ca^{2+} ion bound to its EF-hand within the ER lumen under basal conditions with the ER Ca^{2+} store filled. Ion channels and functions include (clockwise from right): Kv1.3 maintains the resting membrane potential and participates in RVD; Cl_{swell} triggers RVD by opening in response to cell swelling; KCa3.1 hyperpolarizes the membrane potential when cytosolic Ca^{2+} rises; Orai1 embodies the pore-forming subunit of the CRAC channel and is activated by STIM1 following ER Ca^{2+} store depletion (dotted line); TRPM7, activated by PIP_2 and inhibited by Mg^{2+} inside, may regulate Mg^{2+} homeostasis in the cell. Proximal signaling events inside the cell following presentation of antigen include the following (counterclockwise from top right): TCR engagement of peptide–MHC, activation of tyrosine kinases (TK: Lck, Fyn, and ZAP-70), and phospholipase-C-γ (PLCγ), resulting in the cleavage of PIP_2 to generate the second messengers IP_3 and DAG; IP_3-induced Ca^{2+} release; depletion-induced mobilization of STIM1 and activation of Ca^{2+} influx through Orai1 subunits. Post-Ca^{2+} events include activation of KCa3.1 via prebound CaM, activation of calcineurin via CaM, accumulation of dephosphorylated NFAT subunits in the nucleus, binding to DNA promoter regions, and altered gene expression. Functionally significant changes in ion channel expression and Ca^{2+} signaling are indicated by arrows corresponding to changes during acute and chronic activation. TCR, T-cell receptor; STIM, stromal interacting molecule; RVD, regulatory volume decrease; Cl_{swell}, swelling-activated Cl^- current; PIP, phosphatidylinositol 4,5-bisphosphate; MHC, major histocompatibility complex; DAG, diacylglycerol; CaM, calmodulin.

reporter T-cell line (192). By monitoring the history of Ca^{2+} oscillations in single NFAT reporter T cells, followed by a snapshot of gene expression at varying times, it became clear that the frequency of Ca^{2+} oscillations positively correlated with the probability of gene expression, even when the averaged Ca^{2+} responses showed little difference. Ca^{2+} oscillations were not required, however. Varying the ionic gradients to clamp cytosolic Ca^{2+} concentration to different, steady levels permitted the time course of gene expression to be determined quantitatively. NFAT-driven expression begins after an initial delay of 1 h followed by an exponential increase to a maximum after 5 h. Sustained Ca^{2+} signals evoked by thapsigargin alone were sufficient to drive NFAT reporter gene expression in about a third of cells, provided Ca^{2+} was elevated above 1 μM. Interestingly, protein kinase C (PKC) stimulation strongly potentiated the Ca^{2+} dependence of gene expression, making it possible for a smaller steady rise in Ca^{2+} to 300 nM to drive gene expression effectively in the majority of cells (192). Moreover, a hierarchy of signaling pathways was defined in which elevated Ca^{2+} was absolutely required: PKC stimulation alone had no effect, elevation of cAMP was shown to be inhibitory for Ca^{2+}-stimulated gene expression, but cAMP inhibition could be overridden by concomitant activation of PKC (192). The relationship between Ca^{2+} dynamics and different gene expression pathways was further examined by Lewis and colleagues (193, 194), also using thapsigargin to clamp cytosolic Ca^{2+} to varying levels and oscillatory frequencies. Rapid oscillations efficiently produced gene expression via NFAT, Oct/OAP, or NF-κB, whereas infrequent oscillations were effective in driving only NF-κB. Ca^{2+} oscillations may serve to drive gene expression efficiently but without the dangerous consequence for cells of prolonged elevation of cytosolic Ca^{2+}. As described elsewhere in this volume, gene expression array profiling of control and SCID patient T cells reinforced the central role of Ca^{2+} signaling and CRAC channel function in T-cell activation (195).

Channels at the immunological synapse

Both Kv1.3 and KCa3.1 in T cells are recruited to the immunological synapse during antigen presentation (15, 196–200). More recently, we showed that STIM1 and Orai1 also re-localize at the DC interface within 5 min of contact, resulting in localized Ca^{2+} influx into the synaptic region of the T cell (91). Channel function and Ca^{2+} signaling do not appear important for initial formation of the immunological synapse, as inhibiting either Kv1.3 (15, 197) or CRAC channels (91) did not prevent molecular clustering in the contact zone. However, the long-term stability of the immunological synapse was shown to be compromised by blocking Ca^{2+} entry in combination with increasing intracellular Ca^{2+} buffering (184, 201), although the initial contact formation and redistribution of CD3 to the contact area was not affected (201). Thus, it is possible that the recruitment of CRAC channels to the immunological synapse where receptors, adhesion molecules, and costimulatory molecules also accumulate is important for long-term Ca^{2+}-dependent regulation of the signaling events triggered upon antigen presentation.

The Ca^{2+} signal typically detected with indicator dyes is a global Ca^{2+} signal throughout the cell. As Ca^{2+} diffuses rapidly in the cytosol, it distributes uniformly (184). Fast Ca^{2+} diffusion combined with limited resolution of the microscope make it difficult to detect localized Ca^{2+} entry without resorting to a trick. Local Ca^{2+} entry in the T cell adjacent to the DC contact zone was revealed by loading the T cells with a fast Ca^{2+} indicator dye (fluo-4) together with a large amount of a slow Ca^{2+} buffer (EGTA) (91). Localized Ca^{2+} entry into the T cell at the synapse was then revealed as the fast indicator dye could catch the Ca^{2+} ions as they entered locally before they were buffered. A persistent and localized Ca^{2+} entry was observed minutes after the initial contact with APC and is therefore unlikely to involve signal initiation by IP_3 generation. In a previous Ca^{2+} imaging study from Roger Tsien's laboratory (178), the Ca^{2+} signal was initiated at the rear end of cytotoxic T lymphocytes (CTLs) engaging targets, but the gradient did not persist. The rear-to-front gradient lasted only seconds and was replaced by a global Ca^{2+} signal; the transient Ca^{2+} gradient, which was not seen in other Ca^{2+} imaging studies (182, 184), may have resulted from localized IP_3 generation to initiate the Ca^{2+} signal near the uropod of the polarized CTL following contact with the target. A polarized distribution of STIM1 and Orai1 at caps and in the uropod region of T cells has also been reported (92), and this may promote signal initiation under some circumstances.

What purpose might be served by the localization of ion channels to the immunological synapse? Compared with a neuron having a long axon with cable properties, T cells are nearly spherical and therefore isopotential, particularly when rounded up in contact with an APC. Thus, the accumulation of K^+ and Ca^{2+} channels at the immunological synapse cannot convey electrical signals away from the synapse in a manner analogous to a neuronal synapse or the end plate of a neuromuscular junction. Here, we speculate on several possible functions related to (i) localized Ca^{2+} influx producing intracellular domains of high Ca^{2+}, (ii) localized Ca^{2+} depletion in the synaptic cleft, (iii) localized K^+ efflux inducing K^+ accumulation in the synaptic cleft, and (iv) molecular aggregations.

(i) A localized Ca^{2+} influx at the synapse would be expected to produce a high localized Ca^{2+} concentration within nanodomains immediately inside the T cell next to the APC. The local Ca^{2+} signal adjacent to clusters of Orai1 (CRAC) channels could result in very high micromolar levels of free Ca^{2+} concentration, in turn triggering localized activation of enzymes or localized Ca^{2+} binding to numerous substrates, including elements linked to the cytoskeleton. This could assist in Ca^{2+} signal modulation by producing fast or slow local inactivation of CRAC channels (202, 203) or the dissolution of STIM1 puncta (204). It could also serve to stabilize the synapse (201) or perform other functions that require occupancy of a relatively low affinity Ca^{2+} binding site. Mitochondria accumulate in the subsynaptic region of the T cell and help to maintain CRAC current by removing Ca^{2+} from the region (205–208).

(ii) Ca^{2+} entry could also produce significant localized depletion of extracellular Ca^{2+} from within the cleft between the T cell and the APC. The volume within this region of contact is unknown but can be estimated by multiplying the combined surface areas of central (c-) and peripheral (p-) supramolecular activation cluster (SMAC) zones, approximated here to be on the order of 10 μm^2, by the distance between the T cell and the APC. The minimal average width of the synaptic cleft has been estimated using electron microscopy to be 20 nm between a T cell and a DC (209) and on the same order for NK target cell synapses (210), close enough for direct molecular interactions including the engagement of peptide–major histocompatibility complex (MHC) by TCR, as well as integrins (ICAM1-LFA), costimulatory molecules (CD80/86-CD28), and other direct interactions in the synapse. Previous estimates, based on size exclusion of membrane proteins, reached a similar conclusion that the cleft width is between 15 and 40 nm (211, 212). The high density

of such proteins interacting in the gap could greatly reduce the effective diffusion coefficient of ions in the synaptic cleft, either by displaying ionic binding sites or by simply occupying a significant amount of space. The actual contact zone is multifocal, with regions of extremely close membrane apposition interspersed in a wider synaptic zone (209). However, for simplicity we considered the cleft to be a cylinder and estimated the volume within the synaptic cleft as 0.2 fl (1 fl = 10^{-15} l). Given these dimensions and neglecting diffusion out of the synaptic cleft, a few simple calculations lead to the conclusion that the flux of Ca^{2+} through CRAC channels into the cell could severely deplete the extracellular Ca^{2+} concentration locally within the synaptic cleft, particularly if diffusion of Ca^{2+} from the periphery is slowed by molecules within the cleft. As a rough estimate, to obtain micromolar levels of free Ca^{2+} throughout a T cell having a picoliter volume (a reasonable estimate for Ca^{2+} levels and volume of a T-cell blast following TCR engagement; both would be smaller in a resting T cell) and with buffer capacity typical of cytoplasm of 50 bound Ca^{2+} ions for each free Ca^{2+} ion, at least 3 million Ca^{2+} ions would have to enter the cell. If taken away from a volume of 0.2 fl, an entirely hypothetical depletion of 250 mM could occur, i.e. clearly more than sufficient to completely deplete the cleft of all Ca^{2+} ions. Of course, this calculation does not consider Ca^{2+} diffusion back into the cleft from the periphery of the p-SMAC (at a rate that is difficult to assess) and Ca^{2+} pumping out of the cell (we do not know where the pumps are localized), but the 'back of the envelope' order-of-magnitude calculation shows that significant depletion of Ca^{2+} within the cleft is possible. This could have several interesting effects, including attenuation of Ca^{2+} influx through CRAC channels, increasing electrostatic binding interactions between surface molecules in the T cell and the APC, or increasing the local negative surface charge within a Debye length of the membrane (expected to mimic depolarization from the standpoint of voltage sensors in the membrane).

(iii) As a result of Kv1.3 or KCa3.1 accumulation in the synapse, efflux of K^+ from the T cell into the cleft would be expected to produce a localized increase in extracellular K^+ concentration, and this could result in plasma membrane depolarization of the T cell or the APC. Local extracellular K^+ accumulation due to ion channel activity are known to have important consequences in nerve and muscle cells. As a historical note, in his last experimental paper Katz (213) showed exactly this effect in the synaptic cleft of a neuromuscular junction. Again, one can estimate by how much extracellular K^+ concentration would change in the immunological synapse as a result of K^+ channel activity. Suffice it to say that if a single Kv1.3 channel (or a KCa3.1 channel of similar single-channel conductance) were open for 1 s, 2 million K^+ ions would move across the membrane into the synaptic cleft. Given the assumed dimensions of the cleft and if diffusion out of the cleft is restricted, then a single open K^+ channel would increase the local K^+ concentration from a basal value of 4 to 20 mM in 1 s. To produce significant depolarization of the T cell, the local K^+ concentration would need to increase to more than 8 mM, as the resting potential is already depolarized relative to the equilibrium potential for K^+ ions. The membrane potential would then deviate toward a new equilibrium potential determined by local extracellular K^+ concentration in the cleft, and this deviation would depend upon the relative numbers of K^+ channels exposed to normal external K^+ and those exposed to locally elevated K^+. As both Kv1.3 and KCa3.1 are mostly in the immunological synapse region, it is not unreasonable to suggest that significant membrane depolarization would occur. These basic calculations show that accumulation of K^+ could be significant and likely to depolarize the membrane potential, but they do not take into account rates of diffusion of K^+ out of the restricted volume (*Fig.* 5).

There could be several interesting effects of K^+ ion accumulation. Direct effects of extracellular K^+ ion on Kv1.3 are well studied – inactivation is reduced and single-channel currents are increased (2). Both of these effects in combination with increased activation of Kv1.3 channels due to depolarization would tend to increase K^+ conductance and would clamp the membrane potential more effectively at a depolarized level and possibly attenuate Ca^{2+} influx through CRAC channels. It is also possible that the APC would depolarize. Any voltage sensors in either the T cell or the APC would be expected to respond, perhaps even non-conducting CaV subunits. CaV subunits could be linked to ryanodine receptors in the ER and cause Ca^{2+} release from internal stores. Although highly speculative, such local depolarizing effects (Ca^{2+} depletion, K^+ accumulation) might cause Ca^{2+} signals that have been seen in dendritic cells during contact with T cells (214). In DCs, even though CaV α-subunits are expressed (215), the major Ca^{2+} influx pathway is the CRAC channel (216). Treves and colleagues (215) have recently found that K^+-induced depolarization activated Ca^{2+} release from internal stores that was blocked by ryanodine, implying voltage coupling from the plasma membrane to the ER Ca^{2+} store or Ca^{2+}-induced Ca^{2+} release, both analogous to excitation–contraction coupling in muscle. Moreover, they found that DC expression of MHC class II nearly doubled within a minute of K^+-induced

depolarization. Further speculation is perhaps unwarranted without additional experiments, but the mechanism outlined here involving K^+ accumulation in the T cell–DC synaptic cleft could call CaV voltage sensors into play, possibly even if they lacked functional pores, and it could enable functionally significant communication from the T cell to the APC and back again by delivering a greater quantity of peptide–MHC to the APC surface.

(iv) As Kv1.3 is in physical association with a large signaling complex (*Fig.* 6), its localization at the immunological synapse promotes the clustering of associated proteins at the synapse. Colocalization of these proteins into a signalosome at the immunological synapse may provide a mechanism to couple external stimuli with intracellular signaling cascades. ZIP is a multi-functional protein (217, 218) that links the Kv1.3 auxiliary subunit Kvβ2 to Lck (15). ZIP binds ubiquitin noncovalently and could affect signal transduction through ubiquitination-mediated protein degradation (219). ZIP also binds to other proteins and may thereby regulate T-cell activation: to ras GTPase-activating protein, a negative regulator of the ras signaling pathway (217, 218), to p38-MAPK and PPARα (220), to TNF receptor-associated factor 6 (221), a regulator of NF-κB activation, and protein kinase Cξ (222). Protein kinase Cξ promotes T-cell polarity and uropod formation during locomotion and dendritic cell scanning (223). The Kv1.3–Kvβ2–ZIP–Lck complex may be targeted under hypoxic conditions leading to reduced T-cell activation. Hypoxia suppresses Kv1.3 through an Lck-mediated mechanism resulting in membrane depolarization and attenuated calcium signaling (224, 225). Hypoxia also enhances the clearance of ZIP proteins (226). Kvβ2 shows structural homology with aldo–keto reductases (227), catalyzes the reduction of a variety of aldehydes and ketones (228), and binds pyridine nucleotides (NADP) with high affinity; moreover, the integrity of the $NADP^+$ binding pocket is essential for trafficking of Kv1.x channels to the cell surface (229). The C-terminus of Kv1.3 is linked to Lck via a PDZ-domain protein called hDlg (also referred to as SAP97) (230). hDlg binds to GAKIN, a member of the family kinesin motor proteins, and the hDlg–GAKIN complex may contribute to the reorganization of the cortical cytoskeleton during activation (231). Kv1.3 may also function as a physical bridge between β1-integrin (232) and the signaling molecules described above, thereby functionally coupling external integrin interactions to signal transduction internally. Such coupling could be enhanced by local accumulation of extracellular K^+ in the synaptic cleft, as elevated extracellular K^+ has been reported to activate T-cell β1-integrin and to induce integrin-mediated adhesion (232). Finally, the close proximity of Kv1.3 to its partners within the signaling complex affords a mechanism for channel regulation. Triggering through the Fas/apoptotic receptor leads via Lck to tyrosine phosphorylation of Kv1.3, resulting in channel suppression (233, 234). In other tissues (e.g. olfactory bulb) phosphorylation of Kv1.3 at Y449 (in the C-terminus) and/or YYY 11-113 in the N-terminus contributes to channel suppression (235, 236). In summary, Kv1.3 may serve as a scaffold that couples the T-cell antigen receptor complex to β1 integrin and to intracellular signaling molecules that modulate the activation process.

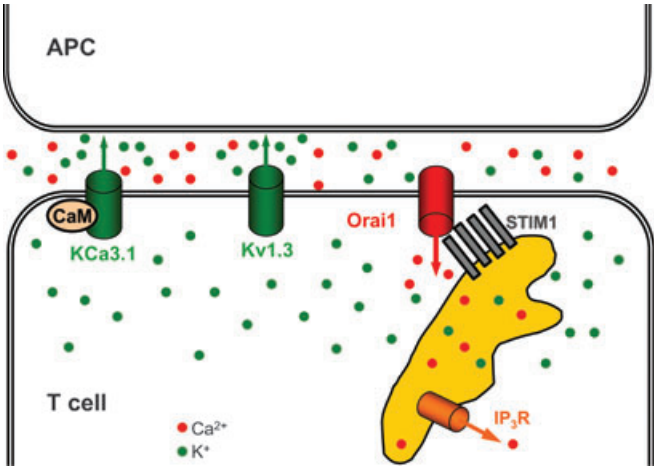

***Fig.* 5. Ion channels at the immunological synapse.** Kv1.3, KCa3.1, STIM1, Orai1 are shown diagramatically in relation to the T cell–APC interface. Same color codes for ions and channels as in *Fig.* 4. During Ca^{2+} signaling, Ca^{2+} may be depleted and K^+ may accumulate in the synaptic cleft between the T cell and the APC. STIM, stromal interacting molecule; APC, antigen-presenting cell.

The KCa3.1/CaM channel complex is physically coupled to nucleoside diphosphate kinase B (NDPK-B) (also referred to as nm23-H2) and histidine phosphatase (PHPT-1) (55, 56). Both proteins modulate KCa3.1 function by phosphorylating/dephosphorylating His^{358} in the C-terminus of the channel, and both may cluster at the immunological synapse together with KCa3.1. At the immunological synapse, NDPK-B may link KCa3.1 and β1-integrin through its interaction with integrin cytoplasmic domain-associated protein 1alpha (ICAP-1α), a protein that binds to the intracellular portion of β1-integrin (237) (*Fig.* 6).

Role of K^+ channels in lymphocyte activation

In the 1980s, several groups showed that chemically diverse blockers of the Kv1.3 channel inhibit mitogen-induced T-cell proliferation, protein synthesis, IL-2 production, allogeneic mixed lymphocyte response (MLR), autologous MLR but not

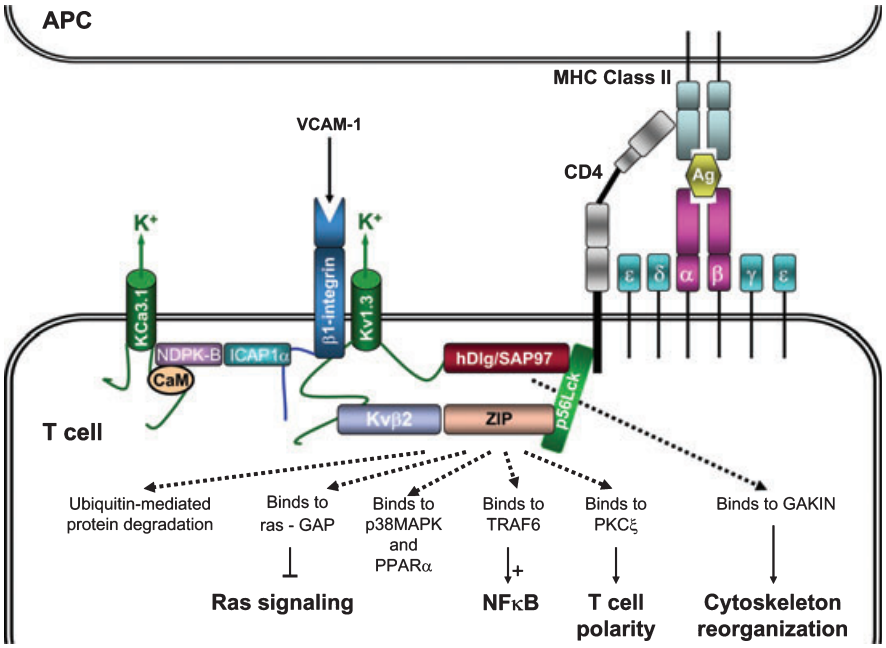

***Fig. 6.* K^+ channel-associated proteins at the immunological synapse.** The last three residues in the C-terminus of Kv1.3 bind the PDZ-domain protein hDlg [also known as synapse-associated protein 97 (SAP97)], which in turn binds to Lck. The T1 (tetramerization) domain in the N-terminus of Kv1.3 binds to Kvβ2. Kvβ2 may link cellular metabolic activity and redox state with electrical and calcium signaling in lymphocytes. Kvβ2 also serves as a bridge with ZIP (Sequestosome 1/p62), which binds to Lck in a phosphotyrosine-independent fashion, and to several other signaling proteins. Immunoprecipitation studies show that Kv1.3 and β1-integrin are physically associated, although the precise interaction sites have not been determined. The sites of interaction between KCa3.1 and NDPK-B also have not been identified, but, because NDPK-B phosphorylates a histidine residue in the C-terminus of the channel, we have shown KCa3.1's C-terminus interacting with NDPK-B. NDPK, nucleoside diphoshate kinase.

expression of IL-2 receptors (3, 18, 238–240). A parallel potency sequence was observed for K_V channel blockade and T-cell suppression: TEA < 4AP < diltiazem < quinine < verapamil. Of interest was the discovery that classical 'Ca^{2+} channel antagonists' (dilitiazem and verapamil) inhibit T-cell activation by blocking K_V channels (18, 19). In the late 1980s, charybdotoxin, a 37-residue peptide from scorpion venom, was discovered to block Kv1.3 (22, 24) and also to suppress IL-2 production and proliferation of human T cells (239). Kv1.3 peptide inhibitors from scorpion venom (noxiustoxin and margatoxin), and from sea anemones (ShK), were shown to suppress T-cell activation and Ca^{2+} signaling in human T cells (59, 166, 241, 242). Collectively, these studies established an essential role for the Kv1.3 channel in T-cell proliferation.

What is the mechanism of suppression? A 24-h delay in the addition of the Kv1.3 blockers reduces the effectiveness of T-cell suppression (18), suggesting that inhibition of an early event during T-cell activation is required for the immunosuppressive effect of the blockers. As exogenous recombinant IL-2 reverses inhibition by Kv1.3 blockers (18, 239), attention was focused on the signaling events that led to IL-2 production. Studies with peptide toxin inhibitors of Kv1.3 revealed that the anti-proliferative effect of the blockers was due to membrane depolarization and consequent reduced calcium entry (165, 166, 242, 243). Subsequent studies with other more selective Kv1.3 blockers or genetic silencing of Kv1.3 confirmed the role of membrane depolarization and attenuated calcium signaling in mediating the immunosuppressive effect of Kv1.3 blockers (15, 59, 241, 244, 245).

Changes in the ion channel phenotype in lymphocyte subsets

The expression pattern of ion channels in a particular T cell defines its channel phenotype. Expression levels can vary dramatically in different cell types, subsets, states of activation, and states of secondary differentiation. Further adding to the complexity, human and murine immune responses and lymphocytes differ in their functional characteristics (246). Even rat and mouse have significant differences in channel phenotypes (247). With several channels to distinguish, it is not surprising that we have an incomplete data set. Yet, some functionally important generalizations regarding the phenotype of the two main lymphocyte K^+ channels have emerged. Moreover, recent studies have shown that CRAC channels (STIM1 and Orai1,2,3) may also exhibit increased expression

levels during lymphocyte activation and these may also have functional consequences for Ca^{2+} signaling and implications for immunotherapy.

K^+ channel phenotype: of mice and men (and rats)

Kv1.3 and KCa3.1 expression levels vary during T-cell activation and differentiation into memory T cells (*Fig. 7*). Under basal conditions, quiescent naive ($CD4^+$ or $CD8^+$ $CCR7^+CD45RA^+$) human T cells express predominantly voltage-gated Kv1.3 channels at levels corresponding to a few hundred functional channels per cell (2, 3, 248). By contrast, quiescent mouse and rat T cells have much lower levels of voltage-gated K^+ channel activity at fewer than 10 channels per cell (40, 249). Within a day of activation, the expression of Kv1.3 increases in mouse and rat naive T cells to levels seen in human T cells (approximately 300–500 Kv1.3 channels per cell) (40, 248–250). Consistent with a moderate to high level of expression when cells are proliferating, Kv1.3 is also expressed at a higher level in rapidly proliferating mouse thymocyte subsets than in mature single positive mouse subsets (147, 251). Expression of Ca^{2+}-activated KCa3.1 channels increases dramatically upon activation of human, mouse, and rat naïve T cells from fewer than 10 channels per cell in quiescent cells to an average of approximately 500 channels per cell (40, 50, 59). Increased KCa3.1 expression is due to transcriptional activation of Ikaros and AP-1 sites on the KCa3.1 promoter and new synthesis of KCa3.1 channel protein. New transcripts are detectable within 3–6 h of activation (59), and new channels are fully functional within a day.

During an immune response, two types of memory T cells are formed: long-lived central memory (T_{CM}) T cells ($CD4^+$ or $CD8^+CCR7^+CD45RA^-$) and effector-memory (T_{EM}) cells ($CD4^+$ or $CD8^+CCR7^-CD45RA^-$). An important difference between these two memory subsets is the K^+ channel expression pattern. Quiescent human T_{CM} and T_{EM} cells express approximately 300 Kv1.3 channels per T cell along with 10–20 KCa3.1 channels. Upon activation, human T_{CM} cells, like naive T cells, upregulate KCa3.1 when they change into T_{CM} effectors, whereas T_{EM} cells upregulate Kv1.3 (approximately 1500 Kv1.3 channels per cell) when they become T_{EM} effectors (15, 248). Rat T_{CM} effectors and T_{EM} effectors exhibit the same channel pattern as their human counterparts (40, 247).

The differences in K^+ channel expression in $CCR7^+$ and $CCR7^-$ T cells parallel the cells' vulnerability to specific channel blockade. First, resting T cells are sensitive to Kv1.3 channel blockade (18). In our studies in the early 1980s, we reported that Kv1.3 blockers suppressed mitogen-stimulated human T-cell activation at concentrations required to block more than 90% of Kv1.3 channels (18). Those studies used pooled T cells, and it is likely that naive and T_{CM} cells in the pool escaped Kv1.3 blocker-inhibition during the 72-h assay contributing to the high IC_{50} value required for immunosuppression. Another factor that contributed to the requirement for high inhibitor concentrations was the strength of the activation stimulus; potent activation stimuli override the effect of Kv1.3 blockers. Additionally, naive cells may have 'spare' Kv1.3 channels and require a greater percent inhibition to depolarize the membrane potential than in T_{EM} cells. Activated naive and T_{CM} cells with high levels of KCa3.1 acquire sensitivity to KCa3.1 blockade (59, 248). Moreover, in activated naive and T_{CM} blasts with upregulated KCa3.1 channels and in Jurkat T cells with KCa2.2 channels, pharmacological blockade and dominant-negative suppression or overexpression showed that Ca^{2+}-activated K^+ channels may play a more important role in Ca^{2+} signaling than Kv1.3 (181). Sensitivity to Kv1.3 blockade returns in chronically activated T_{EM} cells expressing high numbers of Kv1.3 channels (40, 248). This switch in K^+ channel phenotype in relation to regulation of membrane potential during calcium signaling may explain these observed changes. A counterbalancing efflux of K^+ is needed to sustain Ca^{2+} influx, and either channel can perform this function. Kv1.3 channels regulate membrane potential and calcium signaling in all resting T cells, but when cells activate into naive effector and T_{CM} effector cells, KCa3.1 takes over this role. T_{EM} cells depend on Kv1.3 channels to regulate membrane potential and calcium signaling in the resting and effector stages. Consequently, Kv1.3-specific blockers suppress antigen-induced activation of naive and T_{CM} cells, but these cells rapidly escape Kv1.3 inhibition by upregulating KCa3.1 and become sensitive to KCa3.1 blockers. By contrast, T_{EM} cells remain sensitive to inhibition by Kv1.3 blockers when they transit from quiescent to T_{EM} effector cells and also when T_{EM} effectors undergo further activation (15, 248).

Mouse T cells exhibit a significantly different K^+ channel expression pattern which, unfortunately, precludes their use as a model to evaluate pharmacological inhibitors. Mouse T cells express a variety of different K^+ channels in resting cells (Kv1.1, Kv1.3, Kv1.6, and Kv3.1), and are also distinctly different in the persistence of high KCa3.1 expression in chronically activated T_{EM} cells. Consequently, mouse T_{EM} cells can escape from the inhibition of Kv1.3 because they still express KCa3.1 to counterbalance Ca^{2+} influx through CRAC channels. KCa3.1 blockade is effective in experimental autoimmune encephalitis (EAE) in mouse (252), unlike in rats or humans.

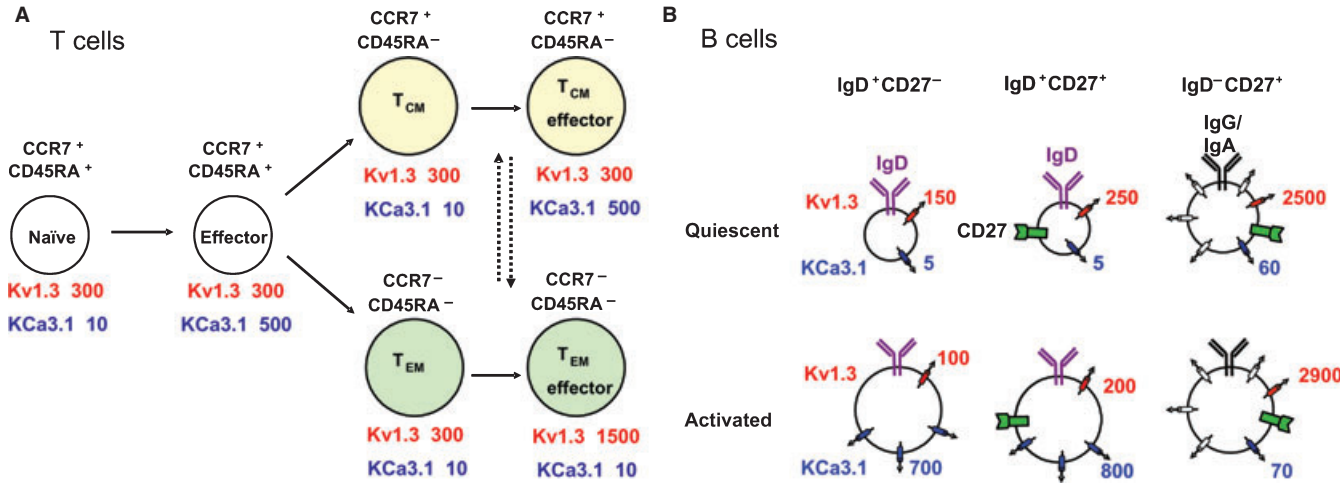

***Fig. 7.* Changes in K^+ channel expression during activation.** The average number of functional Kv1.3 and KCa3.1 channels in individual T or B cells is shown. (A) $CD4^+$ or $CD8^+$ T cells were isolated from human peripheral blood and immunostained with antibodies specific to CCR7 and CD45RA. Naive ($CCR7^+CD45RA^+$), central memory T_{CM} ($CCR7^+CD45RA^-$) and effector memory T_{EM} ($CCR7^-CD45RA^-$) T cells were visualized by fluorescence microscopy and single-cell patch clamp studies were performed on T cells belonging to specific subsets. In other experiments, $CD4^+$ or $CD8^+$ T cells from human peripheral blood were stimulated for 48 h with anti-CD3 or PMA + ionomycin, immunostained, and activated cells (enlarged) corresponding to each of the subsets described above were patch clamped. The Kv1.3 and KCa3.1 channels were identified by their unique biophysical and pharmacological fingerprint. The numbers of functional channels/cell were determined by dividing the total Kv1.3 or KCa3.1 current with the single-channel conductance for each channel. Quiescent naive, T_{CM} and T_{EM} cells exhibited a similar K^+ channel expression pattern with 300 Kv1.3 and 10–20 KCa3.1 channels. Following activation, $CCR7^+$ T cells of the $CD4^+$ and $CD8^+$ lineages (naive effector/T_{CM} effector) upregulated the calcium-activated KCa3.1 channel, whereas $CCR7^-CD4^+$ and $CCR7^-CD8^+$ T_{EM} effectors upregulated Kv1.3 channels. (B) B cells were isolated from human peripheral blood, immunostained with antibodies specific to IgD and CD27, and the different subsets (IgD^+CD27^-: naive; IgD^+CD27^+: early memory; IgD^-CD27^+: class-switched late memory) were analyzed by single-cell patch clamp. In other experiments, isolated B cells were stained with antibodies specific to IgG or IgA together with CD27 and the IgG^+CD27^+ or IgA^+CD27^+ class-switched memory B cells were patch clamped. PMA, phorbol 12-myristate 13-acetate.

An additional change in K^+ channel expression takes place as mouse T cells differentiate to become Th1 cells that secrete IL-2 and IFN-γ or Th2 cells that are specialized for secretion of IL-4, IL-5, and IL-10 (253). Ca^{2+} influx and CRAC channel activity were shown to be the same in both Th1 and Th2 cells. Moreover, Kv1.3 function was also unchanged. However, Ca^{2+}-activated K^+ current attributable to KCa3.1 was significantly higher in Th1 compared with that in Th2 cells, and this expression difference corresponded to the increased Ca^{2+} signal of Th1 cells, as also reported by Allen and colleagues (254, 255). Pharmacological blockade of KCa3.1 reduced Ca^{2+} responses in Th1 cells but not to the level of Th2 cells (253). By analyzing Ca^{2+} clearance in the absence of Ca^{2+} influx, it was found that Th2 cells extrude Ca^{2+} more rapidly than Th1 cells. The combination of faster clearance and reduced KCa3.1 activity accounts for the lower Ca^{2+} response of Th2 compared with Th1 cells.

As is the case with T cells, there are dramatic changes in K^+ channel phenotype in B cells during differentiation and activation (*Fig. 7*). Quiescent naive human B cells ($CD27^-IgD^+$) and early memory B cells ($CD27^+IgD^+$) start with lower levels of Kv1.3 and KCa3.1 channels, but, like their T-cell counterparts (naive and T_{CM} cells), they upregulate KCa3.1 upon activation (256). In this study, we also showed that late memory cells of the T (T_{EM}) and B (class-switched) lineage upregulate Kv1.3 instead of KCa3.1 when activated. Resting class-switched memory B cells ($CD27^+IgD^-IgG^+$ or IgA^+) express much higher Kv1.3 levels than quiescent T_{EM} cells and enhance Kv1.3 levels further after activation (256). Earlier studies on mixed pools of B-cell subsets found increases in both Kv1.3 and KCa3.1 levels after activation (257, 258); they were most likely detecting activation-induced increases in KCa3.1 in naive/early memory B cells and Kv1.3 in late class-switched memory B cells.

Pharmacological sensitivity again parallels K^+ channel phenotype in B cells. In 1990, non-selective Kv1.3 blockers were reported to suppress lipopolysaccharide-induced proliferation of a mixed pool of B-cell subsets (259). More recently, the KCa3.1-specific blocker TRAM-34 was shown to suppress the activation of human IgD^+ B cells (naive or early memory) triggered by anti-CD40 antibody (EC_{50}: 200 nM) or a combination of phorbol 12-myristate 13-acetate (PMA) and ionomycin (EC_{50}: 100 nM) (256). In this study, ShK, at concentrations that block mainly Kv1.3 (10 nM), did not affect the prolifera-

tion of these cells. By contrast, ShK suppressed the activation of class-switched memory B cells stimulated by anti-CD40 antibody or the PMA/ionomycin combination, and TRAM-34 was not effective (256). Thus, KCa3.1 channels are the primary regulators of membrane potential and calcium signaling in effector cells derived from naïve or early memory B or T cells, and Kv1.3 plays this role in effectors generated from late memory B or T cells.

The functional involvement of ion channels extends also to NK cells that also express Kv1.3 channels. NK cells actively patrol lymph nodes and are capable of engaging and destroying foreign cells in swarms that contact and kill the targets (260). During target recognition, CRAC channels are probably activated, producing an oscillatory Ca^{2+} signal (165) that results in secretion of cytolytic granules and elimination of foreign cells. The secretion of cytolytic granules by NK cells and killing of target cells relies on Kv1.3 to sustain the membrane potential (261, 262).

Increases in functional CRAC and K^+ channel expression: a positive feedback loop during T-cell activation

In addition to changes in K^+ channel expression that take place during activation of naive T cells, the CRAC channel components STIM1 and Orai1 and also Orai2 and Orai3 are upregulated at the mRNA level in T-cell blasts within a day of TCR engagement, a change in channel phenotype that lasts for at least 6 days (91). These changes take place in parallel to upregulation of functional KCa3.1 channels and Kv1.3 channels (50, 263). Thus, all three channel types that are involved directly or indirectly in Ca^{2+} signaling in T cells are upregulated upon mitogenic activation following TCR engagement. In RBL cells, functional CRAC channels are expressed at the highest level during G1S and S phases of the cell cycle and are strongly downmodulated during mitosis (127). Upregulation of both CRAC and K^+ channels suggests a possible mechanism by which resting T cells with weak Ca^{2+} signals acquire increased Ca^{2+} responses during the acute activation phase, as observed in comparisons of naive T cells with activated T-cell blasts (91, 124, 165). Upregulation of Orai1 and STIM1 most likely contributes to the enhanced store-operated Ca^{2+} influx in activated T cells, although potential contributions of heteromultimers with Orai2 and Orai3 will need to be evaluated further. Colocalization of CRAC components (Orai1 pore subunit and activator STIM1), Kv1.3, and KCa3.1 channels to the immunological synapse may provide positive feedback involving localized Ca^{2+} entry. Moreover, the rapid upregulation of functional KCa3.1 and CRAC channels would provide feedback for Ca^{2+} signaling evolving over the first few days of activation. One of the implications of Orai1 and STIM1 upregulation in the early stages of an immune response would be to amplify and ensure CRAC channel-mediated Ca^{2+} signaling that is crucial for regulation of gene expression, clonal expansion, and differentiation in T cells.

Visualizing lymphocyte activation and drug action and envisioning the role of ion channels *in vivo*

Introduced to the field of immunology in 2002, two-photon microscopy permits real-time visualization of living cells within their native environment *in vivo* (191, 264, 265). The basal motility pattern of both T and B cells is a stop-and-go three-dimensional random walk. The robust motility of T cells in lymph nodes suggested an antigen-search strategy carried out independently by lymphocytes acting autonomously (266). When specific antigen peptide–MHC is detected, a cascade of events is triggered in T cells that leads to Ca^{2+} signaling and lymphocyte activation; the T-cell response evolves in three distinct phases for both $CD8^+$ cells and $CD4^+$ cells (267, 268). In phase I, T cells make serial, transient contacts with several antigen-bearing DCs. During the initial phase, T cells respond with a Ca^{2+} signal (186, 187), that later results in enhanced gene expression, cytokine secretion, and cell proliferation. In phase II, T cell–DC contact durations increase, leading to prolonged interactions as several T cells cluster around individual DCs. During phase III, enlarged T-cell blasts resume their motility and swarm about DCs, again making serial contacts before undergoing cell division. Meanwhile, after engaging soluble antigen, B cells migrate in a directed manner toward the follicle edge (269), where they appear to capture helper T cells and migrate together as conjugate pairs with the B cell leading the way. The elegant cellular choreography within lymph nodes provides an efficient means for T cells to locate rare antigens in the tissue environment, to activate only when appropriate, and to migrate to the peripheral source of antigen where chemokine secretion coordinates inflammation. In addition, it provides the means for B cells dispersed in the follicle to collect antigen and migrate toward the T cells to obtain help.

Just as there is a complex cellular choreography based upon cell-to-cell contacts and recognition, so too there is choreography at the molecular level in T cells (270–272). We may envision the activity of ion channels as the three phases of T cell–DC interactions evolve. During phase I, the intermittent contacts between T cells and DCs are accompanied by short bursts of Ca^{2+} signaling through CRAC channels. At this time,

Kv1.3 and KCa3.1 expression is quite low, and the Ca^{2+} signal is rather small and spiky (186). Based on *in vitro* studies (91), we propose that the initial Ca^{2+} signals are accompanied by lateral migration of STIM1 and Orai1 to the immunological synapse, serving to focus Ca^{2+} influx at the synapse, but that all channel expression levels are rather low, limiting the size of Ca^{2+} signals in resting cells. During phase II, Kv1.3, KCa3.1, STIM1, and Orai1 would be progressively upregulated, and all of these channel components might in turn participate in three ways: making the Ca^{2+} signal stronger, anchoring T cells at the site of antigen presentation, and perhaps also in stabilizing the synapse. Later, during phase III and as cells undergo rounds of proliferation, the channels undergo cell cycle-dependent changes in expression, including transient downregulation of CRAC channel activity during mitosis. At this time within the draining lymph node and perhaps also at later times as T cells take up residence in distal lymph nodes, the continued high levels of KCa1.3, KCa3.1, STIM1, and Orai1 acutely sensitize T cells to produce a stronger Ca^{2+} signal and enhanced cytokine release in response to DCs bearing antigen. In T cell–B cell conjugate pairs, Ca^{2+} signaling mediated by Orai1 very likely inhibits the motility of T cells, allowing them to be carried off by motile B cells.

Two-photon microscopy is opening a new window for imaging cell motility, interaction dynamics, and drug action *in vivo*. We imaged the cellular responses to two classes of candidate immunosuppressive drugs. In the presence of an $S1P_1$ receptor agonist that mimics the action of FTY-720 in producing sequestration of lymphocytes within the lymph node, resulting in lymphopenia and a paucity of T_{EM} cells in the periphery (273), two-photon imaging within the lymph node revealed lymphocytes logjammed adjacent to lymphatic endothelial cells that line the medullary sinus. Upon removal of the agonist or addition of a competitive antagonist, lymphocytes were imaged traversing into the medullary sinus to egress from the node (274, 275). These studies documented the feasibility of *in vivo* imaging to investigate drug action and highlighted the importance of $S1P_1$ receptor agonism, not antagonism, as being essential for blocking lymphocyte egress to suppress the immune response in peripheral tissues.

In a more recent study, we imaged the behavior of T_{EM} cells during a delayed-type hypersensitivity (DTH) response, as a model for inflammation caused by skin-homing T_{EM} cells (276). $CCR7^-$ effector T cells entered the tissue environment at sites of inflammation. Applying two-photon imaging to the inflamed dermal and subcutaneous tissue, we initially observed T_{EM} cells arrested on tissue antigen-presenting cells. A day later T_{EM} cells were enlarged and actively crawling along collagen fibers. A similar pattern of initial T-cell arrest followed later by active motility was also imaged in spinal cord during invasion by myelin-specific T cells in an EAE model (277). We showed that Kv1.3 channel blockade inhibits the DTH response by specifically targeting activated $CCR7^-$ T effector cells and rendering them immotile in the presence of specific antigen in peripheral tissue. Importantly, the same dosing regimen that was effective in inhibiting motility of T_{EM} cells in peripheral tissue did not affect motility of $CCR7^+$ T cells in lymphoid tissue, nor did it affect motility of bystander cells. Moreover, we showed that K^+ channel blockade can selectively suppress T_{EM} cells in DTH and EAE animal models while sparing the protective acute immune response to influenza and chlamydia infections, allowing these infectious agents to be cleared with normal kinetics (276). Prolonged T_{EM}-cell immobilization in inflamed tissues due to Kv1.3 blockade might prevent $CCR7^-$ effector T cells from receiving activation and survival signals and lead to T_{EM} senescence via cytokine deprivation or the 'death-by-neglect' mechanism.

K^+ channel phenotype and therapeutic action of Kv1.3 blockade in autoimmune disorders

More than 80 different autoimmune diseases are known, and together these affect nearly 120 million people globally. A therapy that functionally inhibits or eliminates disease-specific autoantigen-specific immune responses without compromising the protective immune response is the Holy Grail in the quest to treat autoimmune disease. One approach to achieving this goal is to selectively target T_{EM} cells that have been implicated in the pathogenesis of many autoimmune diseases. Specific inhibitors of Kv1.3 offer an exciting new approach to mute autoreactive T_{EM} cell responses in diverse autoimmune without compromising the protective immune response.

In human patients, K^+ channel phenotyping has particular relevance to autoimmune disorders. In T-cell clones from patients with multiple sclerosis (MS) and type 1 diabetes, Kv1.3 expression was found to be high only in clones of the appropriate antigen specificity (248). For example, in new onset type 1 diabetics, GAD- or insulin-specific patient T cells were $CCR7^-$ T_{EM} effectors that expressed >1000 Kv1.3 channels, whereas myelin-specific T patient cells were $CCR7^+$ T cells exhibiting the Kv1.3 expression pattern of quiescent cells (15). In patients with MS, the converse expression pattern was found (15, 278). In a patient with both MS and type 1 diabetes, Kv1.3 expression was high in both MBP- and GAD-specific T cells (15). MHC-tetramer-sorted GAD65-specific $CD4^+$ T cells from type 1 diabetic subjects were also $CCR7^-$

T_{EM} effector cells expressing high levels of Kv1.3, whereas flu-specific T cells from these patients were $CCR7^+$ with low Kv1.3 levels (15). T cells with the same autoantigen specificities from healthy individuals or patients with type 2 diabetes also expressed low numbers of Kv1.3 channels. In the brain of patients with MS, we found a predominance of $CD3^+/CD4^+$ T cells in the perivenular infiltrate; many of these cells stained positively for Kv1.3 (200). In addition, $Kv1.3^+$ cells were highly evident in the parenchymal infiltrate of the majority of MS plaques. Serial sections through areas of intense Kv1.3 staining on lymphocytes revealed negative CCR7 but positive CCR5 staining on the infiltrating cells (200). There was no expression of Kv1.3 in either white matter or gray matter in normal brain tissue. In a subsequent study, we discovered that T cells from the synovial fluid of affected joints from patients with rheumatoid arthritis (RA) were $CCR7^-$ T cells with elevated Kv1.3 levels, whereas T cells from the synovial fluid of non-autoimmune osteoarthritis patients were $CCR7^+$ T cells with low Kv1.3 (15). Synovial biopsies from the affected RA joints revealed $CD3^+CCR7^-$ T_{EM} cells that stained positively for Kv1.3. Specific Kv1.3 blockers preferentially suppressed the disease-associated autoreactive T_{EM} cells without impacting other subsets in these patients. T_{EM} cells have also been implicated in the pathogenesis of many other autoimmune diseases and chronic graft-versus-host disease as discussed in a previous review (247). Kv1.3 inhibitors may therefore have value in the treatment of diverse autoimmune diseases. In fact, clofazimine, a recently discovered Kv1.3 inhibitor, has been used in the treatment of cutaneous lupus, pustular psoriasis, and chronic graft-versus-host disease (244)

In rats, myelin-specific $CCR7^-$ T_{EM} cells that express high numbers of Kv1.3 channels induce severe EAE following adoptive transfer into healthy rats (40, 279). Furthermore, in these studies, Kv1.3 blockers were shown to suppress myelin antigen-triggered proliferation of these $Kv1.3^{high}$ $CCR7^-$ T_{EM} effectors, and daily administration of Kv1.3 blockers both prevented and effectively treated EAE. In chronic relapsing–remitting EAE induced in rats by immunization with autologous spinal cord in emulsion with complete Freund's adjuvant, T cells in the central nervous system are predominantly $CCR7^-$ T_{EM} effectors during the chronic relapsing stage of disease (276). Consequently, Kv1.3 blockers administered by once-daily subcutaneous injection from the start of symptoms ameliorate relapsing disease by decreasing inflammatory infiltrate and demyelination. T cells in the skin of rats with the DTH response are $CD4^+CCR7^-$ T_{EM} effectors with elevated Kv1.3 expression (15), and, in contact dermatitis, the skin T cells are $CD8^+$ T_{EM} effectors (280). Kv1.3 blockers suppress both DTH and contact dermatitis in rats (15, 49, 276, 279–282). PAP-1 administered topically or systemically reduces contact dermatitis and suppresses IFN-γ and IL-17 production in the inflamed skin (280). Kv1.3 blockers also effectively treat disease in rat models of rheumatoid arthritis (15) and bone resorption due to periodontitis (mediated by T_{EM} cells) (283, 284), and they prevent the spontaneous development of autoimmune diabetes in BB rats (15). In minipigs, the Kv1.3 channel blockers, margatoxin and correolide, suppress DTH to tuberculin, and, 2–3 weeks following the cessation of treatment, DTH could not be elicited by repeat challenge with tuberculin (285, 286). This period of 'remission' by Kv1.3 blocker therapy may be the result of the death-by-neglect mechanism whereby tuberculin-specific skin-homing T_{EM} cells are immobilized and then deleted at the site of DTH. Kv1.3 blockers also suppress the primary but not the secondary antibody response to allogeneic antibody in minipigs (285, 286). Clofazimine, the recently discovered Kv1.3 blocker, prevents rejection of human skin grafts in immunodeficient Pfb-$Rag2^{-/-}$ mice (which lack T, B, and NK cells) following the adoptive transfer of allogeneic human T cells (244). In summary, Kv1.3 blockers have proven efficacy in seven rat models of autoimmune disease (two models of EAE, DTH, contact dermatitis, rheumatoid arthritis, type 1 diabetes, and bone resorption secondary to periodontitis), in a minipig model for DTH and allogeneic antibody responses, and in a SCID-hu mouse model for allogeneic skin graft rejection.

Inhibition of Kv1.3 offers a good approach to modulate pathologic immune responses mediated by autoreactive T_{EM} cells in animal models, but an important issue in developing Kv1.3 blockers as therapeutics is the balance between efficacy and safety. Clofazimine has been used in humans for nearly 70 years. It is generally safe, although it causes reversible skin discoloration in many patients. Prolonged therapy with high concentrations of clofazimine results in the formation of drug crystals in tissues, leading to bullseye retinopathy, vortex keratopathy, enteropathy, splenic infarction, and, in one case, death (287–290). In minipigs, margatoxin and correolide did not cause overt toxicity, although continuous infusion of margatoxin induced mild hypersalivation and decreased appetite, while a higher dose administered as an intravenous bolus resulted in transient hyperactive behavior (286). The selective Kv1.3 blockers (ShK-186, ShK-170, and PAP-1) have been found to be safe in rats and monkeys. They exhibit greater than 10 000-fold selectivity over the HERG channel that underlies many drug-induced cardiac arrhythymias, and ShK-170 did not alter heart rate variability parameters in rats

(279). ShK-170 and PAP-1 were not cytotoxic on a panel of mammalian cells and were negative in the Ames test (49, 279). ShK-170 and ShK-186 administered daily for 2–4 weeks did not cause clinical toxicity and did not change blood counts, blood chemistry, or histopathology of a panel of tissues (15, 279). PAP-1 showed an excellent safety profile in rats administered the drug daily for 6 months and in monkeys (*Macaca mulata*) given the drug daily for a month (291). Importantly, selective Kv1.3 blockers did not compromise the protective immune response to acute viral (influenza) or bacterial (chlamydia) infections at pharmacological doses that ameliorate autoimmune diseases (276). After repeated subcutaneous administration for 28 days, ShK-186 elicited low titer anti-ShK antibodies (15), but these antibodies do not appear to be neutralizing in DTH. The relative safety of Kv1.3 blockers may be due in part to channel redundancy and partly because Kv1.3 blockers may not inhibit Kv1.3-containing heteromultimers (e.g. in the central nervous system) with the same affinity as Kv1.3 homotetramers in T cells. Together, these data suggest that selective Kv1.3 blockers may be excellent candidates for continued development for treatment of autoimmune diseases.

Overview and future directions: opportunities for immunotherapy

T-cell ion channels – STIM1 + Orai1 (CRAC), Kv1.3, KCa3.1 – regulate Ca^{2+} signaling upon TCR engagement. At the molecular level, these are exciting times in the Ca^{2+} signaling field and many detailed questions remain concerning how STIM1 migrates to the plasma membrane and how it activates Orai1 channels to open. At the subcellular level, there are many open questions about the function of synaptic channels in the immune system. At the level of ion channel plasticity, STIM1, Orai1, Orai2, Orai3, and KCa3.1 are all upregulated within a day following TCR engagement, resulting in a stronger Ca^{2+} response upon re-exposure to antigen and a shift in the sensitivity for specific K^+ channel blockade. In only one case (KCa3.1) have promoter mapping studies been conducted. We need to learn more to understand and potentially modulate changes in the channel phenotype in different T-cell subsets and states of activation. Chronic T-cell activation leads to upregulation of Kv1.3 in T_{EM} cells.

Channel blockers that target Kv1.3 or CRAC channels mediate immunosuppressive effects by inhibition of Ca^{2+} signaling, and their actions may be synergistic with existing immunosuppressive compounds. In principle, CRAC channel blockers identified in high-throughput screens could target any of the molecular steps leading from ER Ca^{2+} store depletion to Ca^{2+} influx, including STIM1 sensing of ER luminal Ca^{2+}, STIM1 oligomerization and translocation to the plasma membrane, STIM1 interaction with Orai1 channels and subsequent conformational changes, or the open Orai channel itself. Potent and selective CRAC channel blockers are needed to evaluate potential effects *in vivo*. Orai1 may offer an effective target for transplant rejection but at the risk of inhibiting immune responses to acute infection. Moreover, STIM1 and Orai1 may play important roles in several other cell types, including skeletal and smooth muscle cells as well as other hematopoietic cells (reviewed in 74). Orai2 and Orai3 are also widely distributed in the body and play uncertain functional roles that also need further investigation.

The particular sensitivity to Kv1.3 channel blockade offers opportunities for selective immunomodulation by targeting chronically activated T_{EM} cells, including chronic inflammation and autoimmune disorders. Kv1.3 block by ShK peptide has been validated in seven different animal models for selective block of autoimmune disorders and inflammation mediated by T_{EM} cells. Kv1.3 channel blockade attenuates calcium signaling and inhibits motility of activated T_{EM} cells in peripheral tissues. Further research is needed to determine whether the immotile T effector cells may die of neglect, implying that a relatively short-term or pulsate treatment regimen may be effective for long-term amelioration of autoimmunity. We look forward to the continued use of immuno-imaging methods in the evaluation of channel function *in vivo*.

References

1. Hamill OP, Marty A, Neher E, Sakmann B, Sigworth FJ. Improved patch-clamp techniques for high-resolution current recording from cells and cell-free membrane patches. Pflugers Arch 1981;**391**:85–100.
2. Cahalan MD, Chandy KG, DeCoursey TE, Gupta S. A voltage-gated potassium channel in human T lymphocytes. J Physiol 1985;**358**:197–237.
3. DeCoursey TE, Chandy KG, Gupta S, Cahalan MD. Voltage-gated K^+ channels in human T lymphocytes: a role in mitogenesis? Nature 1984;**307**: 465–468.
4. Matteson DR, Deutsch C. K channels in T lymphocytes: a patch clamp study using monoclonal antibody adhesion. Nature 1984;**307**:468–471.
5. Fukushima Y, Hagiwara S, Henkart M. Potassium current in clonal cytotoxic T

lymphocytes from the mouse. J Physiol 1984;**351**:645–656.
6. Grissmer S, Cahalan M. TEA prevents inactivation while blocking open K^+ channels in human T lymphocytes. Biophys J 1989;**55**:203–206.
7. Panyi G, Sheng Z, Deutsch C. C-type inactivation of a voltage-gated K^+ channel occurs by a cooperative mechanism. Biophys J 1995;**69**:896–903.
8. Nguyen A, et al. Novel nonpeptide agents potently block the C-type inactivated conformation of Kv1.3 and suppress T cell activation. Mol Pharmacol 1996;**50**: 1672–1679.
9. Douglass J, Osborne PB, Cai YC, Wilkinson M, Christie MJ, Adelman JP. Characterization and functional expression of a rat genomic DNA clone encoding a lymphocyte potassium channel. J Immunol 1990;**144**:4841–4850.
10. Grissmer S, et al. Expression and chromosomal localization of a lymphocyte K^+ channel gene. Proc Natl Acad Sci USA 1990;**87**:9411–9415.
11. Attali B, et al. Cloning, functional expression, and regulation of two K^+ channels in human T lymphocytes. J Biol Chem 1992;**267**:8650–8657.
12. Verheugen JA, Vijverberg HP, Oortgiesen M, Cahalan MD. Voltage-gated and Ca^{2+}-activated K^+ channels in intact human T lymphocytes. Noninvasive measurements of membrane currents, membrane potential, and intracellular calcium. J Gen Physiol 1995;**105**:765–794.
13. Maltsev VA. Oscillating and triggering properties of T cell membrane potential. Immunol Lett 1990;**26**:277–282.
14. Chandy KG, Wulff H, Beeton C, Pennington M, Gutman GA, Cahalan MD. K^+ channels as targets for specific immunomodulation. Trends Pharmacol Sci 2004;**25**:280–289.
15. Beeton C, et al. Kv1.3 channels are a therapeutic target for T cell-mediated autoimmune diseases. Proc Natl Acad Sci USA 2006;**103**:17414–17419.
16. Szabo I, et al. Mitochondrial potassium channel Kv1.3 mediates Bax-induced apoptosis in lymphocytes. Proc Natl Acad Sci USA 2008;**105**:14861–14866.
17. Szabo I, et al. A novel potassium channel in lymphocyte mitochondria. J Biol Chem 2005;**280**:12790–12798.
18. Chandy KG, DeCoursey TE, Cahalan MD, McLaughlin C, Gupta S. Voltage-gated potassium channels are required for human T lymphocyte activation. J Exp Med 1984;**160**:369–385.
19. DeCoursey TE, Chandy KG, Gupta S, Cahalan MD. Voltage-dependent ion channels in T-lymphocytes. J Neuroimmunol 1985;**10**:71–95.
20. Han S, et al. Structural basis of a potent peptide inhibitor designed for Kv1.3 channel, a therapeutic target of autoimmune disease. J Biol Chem 2008;**283**:19058–19065.
21. Chandy KG, Cahalan M, Pennington M, Norton RS, Wulff H, Gutman GA. Potassium channels in T lymphocytes: toxins to therapeutic immunosuppressants. Toxicon 2001;**39**:1269–1276.
22. Cahalan MD, Lewis RS. Role of potassium and chloride channels in volume regulation by T lymphocytes. Soc Gen Physiol Ser 1988;**43**:281–301.
23. Deutsch C, Price M, Lee S, King VF, Garcia ML. Characterization of high affinity binding sites for charybdotoxin in human T lymphocytes. Evidence for association with the voltage-gated K^+ channel. J Biol Chem 1991;**266**:3668–3674.
24. Sands SB, Lewis RS, Cahalan MD. Charybdotoxin blocks voltage-gated K^+ channels in human and murine T lymphocytes. J Gen Physiol 1989;**93**: 1061–1074.
25. Garcia-Calvo M, et al. Purification, characterization, and biosynthesis of margatoxin, a component of Centruroides margaritatus venom that selectively inhibits voltage-dependent potassium channels. J Biol Chem 1993;**268**:18866–18874.
26. Alessandri-Haber N, et al. Mapping the functional anatomy of BgK on Kv1.1, Kv1.2, and Kv1.3. Clues to design analogs with enhanced selectivity. J Biol Chem 1999;**274**:35653–35661.
27. Pennington MW, et al. Chemical synthesis and characterization of ShK toxin: a potent potassium channel inhibitor from a sea anemone. Int J Pept Protein Res 1995;**46**:354–358.
28. Kalman K, et al. ShK-Dap22, a potent Kv1.3-specific immunosuppressive polypeptide. J Biol Chem 1998;**273**:32697–32707.
29. Hanson DC, et al. UK-78,282, a novel piperidine compound that potently blocks the Kv1.3 voltage-gated potassium channel and inhibits human T cell activation. Br J Pharmacol 1999;**126**:1707–1716.
30. Wanner SG, et al. WIN 17317-3, a new high-affinity probe for voltage-gated sodium channels. Biochemistry 1999;**38**:11137–11146.
31. Gradl SN, Felix JP, Isacoff EY, Garcia ML, Trauner D. Protein surface recognition by rational design: nanomolar ligands for potassium channels. J Am Chem Soc 2003;**125**:12668–12669.
32. Ehring GR, et al. A nongenomic mechanism for progesterone-mediated immunosuppression: inhibition of K^+ channels, Ca^{2+} signaling, and gene expression in T lymphocytes. J Exp Med 1998;**188**:1593–1602.
33. Baell JB, et al. Khellinone derivatives as blockers of the voltage-gated potassium channel Kv1.3: synthesis and immunosuppressive activity. J Med Chem 2004;**47**:2326–2336.
34. Harvey AJ, Baell JB, Toovey N, Homerick D, Wulff H. A new class of blockers of the voltage-gated potassium channel Kv1.3 via modification of the 4- or 7-position of khellinone. J Med Chem 2006;**49**: 1433–1441.
35. Lanigan MD, Kalman K, Lefievre Y, Pennington MW, Chandy KG, Norton RS. Mutating a critical lysine in ShK toxin alters its binding configuration in the pore-vestibule region of the voltage-gated potassium channel, Kv1.3. Biochemistry 2002;**41**:11963–11971.
36. Aiyar J, Rizzi JP, Gutman GA, Chandy KG. The signature sequence of voltage-gated potassium channels projects into the external vestibule. J Biol Chem 1996;**271**: 31013–31016.
37. Rauer H, et al. Structure-guided transformation of charybdotoxin yields an analog that selectively targets Ca^{2+}-activated over voltage-gated K^+ channels. J Biol Chem 2000;**275**:1201–1208.
38. Rauer H, Pennington M, Cahalan M, Chandy KG. Structural conservation of the pores of calcium-activated and voltage-gated potassium channels determined by a sea anemone toxin. J Biol Chem 1999;**274**:21885–21892.
39. Aiyar J, et al. Topology of the pore-region of a K^+ channel revealed by the NMR-derived structures of scorpion toxins. Neuron 1995;**15**:1169–1181.
40. Beeton C, et al. Selective blockade of T lymphocyte K^+ channels ameliorates experimental autoimmune encephalomyelitis, a model for multiple sclerosis. Proc Natl Acad Sci USA 2001;**98**:13942–13947.
41. Mouhat S, et al. Pharmacological profiling of *Orthochirus scrobiculosus* toxin 1 analogs with a trimmed N-terminal domain. Mol Pharmacol 2006;**69**:354–362.
42. Beeton C, et al. A novel fluorescent toxin to detect and investigate Kv1.3 channel up-regulation in chronically activated T lymphocytes. J Biol Chem 2003;**278**: 9928–9937.
43. Wulff H, Zhorov BS. K^+ channel modulators for the treatment of neurological disorders and autoimmune diseases. Chem Rev 2008;**108**:1744–1773.
44. Hanner M, et al. Binding of correolide to the K(v)1.3 potassium channel: characterization of the binding domain by site-directed mutagenesis. Biochemistry 2001;**40**:11687–11697.
45. Pegoraro S, et al. Inhibitors of potassium channels KV1.3 and IK-1 as immunosup-

pressants. Bioorg Med Chem Lett 2009;**19**:2299–2304.
46. Dreker T, Grissmer S. Investigation of the phenylalkylamine binding site in hKv1.3 (H399T), a mutant with a reduced C-type inactivated state. Mol Pharmacol 2005;**68**:966–973.
47. Rauer H, Grissmer S. Evidence for an internal phenylalkylamine action on the voltage-gated potassium channel Kv1.3. Mol Pharmacol 1996;**50**:1625–1634.
48. Rauer H, Grissmer S. The effect of deep pore mutations on the action of phenylalkylamines on the Kv1.3 potassium channel. Br J Pharmacol 1999;**127**:1065–1074.
49. Schmitz A, et al. Design of PAP-1, a selective small molecule Kv1.3 blocker, for the suppression of effector memory T cells in autoimmune diseases. Mol Pharmacol 2005;**68**:1254–1270.
50. Grissmer S, Nguyen AN, Cahalan MD. Calcium-activated potassium channels in resting and activated human T lymphocytes. Expression levels, calcium dependence, ion selectivity, and pharmacology. J Gen Physiol 1993;**102**:601–630.
51. Ishii TM, Silvia C, Hirschberg B, Bond CT, Adelman JP, Maylie J. A human intermediate conductance calcium-activated potassium channel. Proc Natl Acad Sci USA 1997;**94**:11651–11656.
52. Joiner WJ, Wang LY, Tang MD, Kaczmarek LK. hSK4, a member of a novel subfamily of calcium-activated potassium channels. Proc Natl Acad Sci USA 1997;**94**:11013–11018.
53. Logsdon NJ, Kang J, Togo JA, Christian EP, Aiyar J. A novel gene, hKCa4, encodes the calcium-activated potassium channel in human T lymphocytes. J Biol Chem 1997;**272**:32723–32726.
54. Fanger CM, et al. Calmodulin mediates calcium-dependent activation of the intermediate conductance KCa channel, IKCa1. J Biol Chem 1999;**274**:5746–5754.
55. Srivastava S, et al. Histidine phosphorylation of the potassium channel KCa3.1 by nucleoside diphosphate kinase B is required for activation of KCa3.1 and CD4 T cells. Mol Cell 2006;**24**:665–675.
56. Srivastava S, et al. Protein histidine phosphatase 1 negatively regulates CD4 T cells by inhibiting the K^+ channel KCa3.1. Proc Natl Acad Sci USA 2008;**105**:14442–14446.
57. Srivastava S, et al. Phosphatidylinositol-3 phosphatase myotubularin-related protein 6 negatively regulates CD4 T cells. Mol Cell Biol 2006;**26**:5595–5602.
58. Srivastava S, et al. The phosphatidylinositol 3-phosphate phosphatase myotubularin-related protein 6 (MTMR6) is a negative regulator of the Ca^{2+}-activated K^+ channel KCa3.1. Mol Cell Biol 2005;**25**:3630–3638.
59. Ghanshani S, et al. Up-regulation of the IKCa1 potassium channel during T-cell activation. Molecular mechanism and functional consequences. J Biol Chem 2000;**275**:37137–37149.
60. Wulff H, Gutman GA, Cahalan MD, Chandy KG. Delineation of the clotrimazole/TRAM-34 binding site on the intermediate conductance calcium-activated potassium channel, IKCa1. J Biol Chem 2001;**276**:32040–32045.
61. Wulff H, Miller MJ, Hansel W, Grissmer S, Cahalan MD, Chandy KG. Design of a potent and selective inhibitor of the intermediate-conductance Ca^{2+}-activated K^+ channel, IKCa1: a potential immunosuppressant. Proc Natl Acad Sci USA 2000;**97**:8151–8156.
62. Stocker JW, De Franceschi L, McNaughton-Smith GA, Corrocher R, Beuzard Y, Brugnara C. ICA-17043, a novel Gardos channel blocker, prevents sickled red blood cell dehydration in vitro and in vivo in SAD mice. Blood 2003;**101**:2412–2418.
63. Castle NA, London DO, Creech C, Fajloun Z, Stocker JW, Sabatier JM. Maurotoxin: a potent inhibitor of intermediate conductance Ca^{2+}-activated potassium channels. Mol Pharmacol 2003;**63**:409–418.
64. Lewis RS, Cahalan MD. Mitogen-induced oscillations of cytosolic Ca^{2+} and transmembrane Ca^{2+} current in human leukemic T cells. Cell Regul 1989;**1**:99–112.
65. Zweifach A, Lewis RS. Mitogen-regulated Ca^{2+} current of T lymphocytes is activated by depletion of intracellular Ca^{2+} stores. Proc Natl Acad Sci USA 1993;**90**:6295–6299.
66. Hoth M, Penner R. Depletion of intracellular calcium stores activates a calcium current in mast cells. Nature 1992;**355**:353–356.
67. Hoth M, Penner R. Calcium release-activated calcium current in rat mast cells. J Physiol 1993;**465**:359–386.
68. Roos J, et al. STIM1, an essential and conserved component of store-operated Ca^{2+} channel function. J Cell Biol 2005;**169**:435–445.
69. Yeromin AV, Roos J, Stauderman KA, Cahalan MD. A store-operated calcium channel in *Drosophila* S2 cells. J Gen Physiol 2004;**123**:167–182.
70. Liou J, et al. STIM is a Ca^{2+} sensor essential for Ca^{2+}-store-depletion-triggered Ca^{2+} influx. Curr Biol 2005;**15**:1235–1241.
71. Oritani K, Kincade PW. Identification of stromal cell products that interact with pre-B cells. J Cell Biol 1996;**134**:771–782.
72. Manji SS, et al. STIM1: a novel phosphoprotein located at the cell surface. Biochim Biophys Acta 2000;**1481**:147–155.
73. Zhang SL, et al. STIM1 is a Ca^{2+} sensor that activates CRAC channels and migrates from the Ca^{2+} store to the plasma membrane. Nature 2005;**437**:902–905.
74. Cahalan MD. STIMulating store-operated Ca^{2+} entry. Nat Cell Biol. 2009;**11**:669–677.
75. Wu MM, Buchanan J, Luik RM, Lewis RS. Ca^{2+} store depletion causes STIM1 to accumulate in ER regions closely associated with the plasma membrane. J Cell Biol 2006;**174**:803–813.
76. Feske S, et al. A mutation in Orai1 causes immune deficiency by abrogating CRAC channel function. Nature 2006;**441**:179–185.
77. Vig M, et al. CRACM1 is a plasma membrane protein essential for store-operated Ca^{2+} entry. Science 2006;**312**:1220–1223.
78. Zhang SL, et al. Genome-wide RNAi screen of Ca^{2+} influx identifies genes that regulate Ca^{2+} release-activated Ca^{2+} channel activity. Proc Natl Acad Sci USA 2006;**103**:9357–9362.
79. Le Deist F, et al. A primary T-cell immunodeficiency associated with defective transmembrane calcium influx. Blood 1995;**85**:1053–1062.
80. Partiseti M, Le Deist F, Hivroz C, Fischer A, Korn H, Choquet D. The calcium current activated by T cell receptor and store depletion in human lymphocytes is absent in a primary immunodeficiency. J Biol Chem 1994;**269**:32327–32335.
81. Partiseti M, Le Deist F, Hivroz C, Fischer A, Korn H, Choquet D. Defective transmembrane calcium influx demonstrated in a primary immunodeficiency by video-imaging. C R Acad Sci III 1994;**317**:167–173.
82. Picard C, et al. STIM1 mutation associated with a syndrome of immunodeficiency and autoimmunity. N Engl J Med 2009;**360**:1971–1980.
83. Peinelt C, et al. Amplification of CRAC current by STIM1 and CRACM1 (Orai1). Nat Cell Biol 2006;**8**:771–773.
84. Mercer JC, et al. Large store-operated calcium selective currents due to co-expression of Orai1 or Orai2 with the intracellular calcium sensor, Stim1. J Biol Chem 2006;**281**:24979–24990.
85. Prakriya M, Feske S, Gwack Y, Srikanth S, Rao A, Hogan PG. Orai1 is an essential pore subunit of the CRAC channel. Nature 2006;**443**:230–233.
86. Vig M, et al. CRACM1 multimers form the ion-selective pore of the CRAC channel. Curr Biol 2006;**16**:2073–2079.

87. Yeromin AV, Zhang SL, Jiang W, Yu Y, Safrina O, Cahalan MD. Molecular identification of the CRAC channel by altered ion selectivity in a mutant of Orai. Nature 2006;**443**:226–229.
88. DeHaven WI, Smyth JT, Boyles RR, Putney JW, Jr. Calcium inhibition and calcium potentiation of Orai1, Orai2, and Orai3 calcium release-activated calcium channels. J Biol Chem 2007;**282**:17548–17556.
89. Lis A, et al. CRACM1, CRACM2, and CRACM3 are store-operated Ca^{2+} channels with distinct functional properties. Curr Biol 2007;**17**:794–800.
90. Gwack Y, et al. Biochemical and functional characterization of Orai proteins. J Biol Chem 2007;**282**:16232–16243.
91. Lioudyno MI, et al. Orai1 and STIM1 move to the immunological synapse and are up-regulated during T cell activation. Proc Natl Acad Sci USA 2008;**105**:2011–2016.
92. Barr VA, et al. Dynamic movement of the calcium sensor STIM1 and the calcium channel Orai1 in activated T-cells: puncta and distal caps. Mol Biol Cell 2008;**19**: 2802–2817.
93. Calloway N, Vig M, Kinet JP, Holowka D, Baird B. Molecular clustering of STIM1 with Orai1/CRACM1 at the plasma membrane depends dynamically on depletion of Ca^{2+} stores and on electrostatic interactions. Mol Biol Cell 2009;**20**:389–399.
94. Muik M, et al. Dynamic coupling of the putative coiled-coil domain of ORAI1 with STIM1 mediates ORAI1 channel activation. J Biol Chem 2008;**283**:8014–8022.
95. Navarro-Borelly L, Somasundaram A, Yamashita M, Ren D, Miller RJ, Prakriya M. STIM1–Orai1 interactions and Orai1 conformational changes revealed by live-cell FRET microscopy. J Physiol 2008;**586**:5383–5401.
96. Park CY, et al. STIM1 clusters and activates CRAC channels via direct binding of a cytosolic domain to Orai1. Cell 2009; **136**:876–890.
97. Liou J, Fivaz M, Inoue T, Meyer T. Live-cell imaging reveals sequential oligomerization and local plasma membrane targeting of stromal interaction molecule 1 after Ca^{2+} store depletion. Proc Natl Acad Sci USA 2007;**104**:9301–9306.
98. Luik RM, Wang B, Prakriya M, Wu MM, Lewis RS. Oligomerization of STIM1 couples ER calcium depletion to CRAC channel activation. Nature 2008;**454**:538–542.
99. Huang GN, et al. STIM1 carboxyl-terminus activates native SOC, I(crac) and TRPC1 channels. Nat Cell Biol 2006;**8**:1003–1010.
100. Ji W, et al. Functional stoichiometry of the unitary calcium-release-activated calcium channel. Proc Natl Acad Sci USA 2008;**105**:13668–13673.
101. Penna A, et al. The CRAC channel consists of a tetramer formed by Stim-induced dimerization of Orai dimers. Nature 2008;**456**:116–120.
102. Yuan JP, Zeng W, Huang GN, Worley PF, Muallem S. STIM1 heteromultimerizes TRPC channels to determine their function as store-operated channels. Nat Cell Biol 2007;**9**:636–645.
103. Zhang SL, et al. Store-dependent and -independent modes regulating Ca^{2+} release-activated Ca^{2+} channel activity of human Orai1 and Orai3. J Biol Chem 2008;**283**:17662–17671.
104. Muik M, et al. A cytosolic homomerization and a modulatory domain within STIM1 C-terminus determine coupling to ORAI1 channels. J Biol Chem 2009;**284**:8421–8426.
105. Yuan JP, Zeng W, Dorwart MR, Choi YJ, Worley PF, Muallem S. SOAR and the polybasic STIM1 domains gate and regulate Orai channels. Nat Cell Biol 2009;**11**:337–343.
106. Luik RM, Wu MM, Buchanan J, Lewis RS. The elementary unit of store-operated Ca^{2+} entry: local activation of CRAC channels by STIM1 at ER-plasma membrane junctions. J Cell Biol 2006;**174**:815–825.
107. Xu P, Lu J, Li Z, Yu X, Chen L, Xu T. Aggregation of STIM1 underneath the plasma membrane induces clustering of Orai1. Biochem Biophys Res Commun 2006;**350**: 969–976.
108. Mignen O, Thompson JL, Shuttleworth TJ. Orai1 subunit stoichiometry of the mammalian CRAC channel pore. J Physiol 2008; **586**:419–425.
109. Hoffmann EK, Lambert IH, Pedersen SF. Physiology of cell volume regulation in vertebrates. Physiol Rev 2009;**89**: 193–277.
110. Ross PE, Garber SS, Cahalan MD. Membrane chloride conductance and capacitance in Jurkat T lymphocytes during osmotic swelling. Biophys J 1994;**66**:169–178.
111. Lewis RS, Ross PE, Cahalan MD. Chloride channels activated by osmotic stress in T lymphocytes. J Gen Physiol 1993;**101**: 801–826.
112. Lepple-Wienhues A, Szabo I, Laun T, Kaba NK, Gulbins E, Lang F. The tyrosine kinase p56lck mediates activation of swelling-induced chloride channels in lymphocytes. J Cell Biol 1998;**141**:281–286.
113. Ehring GR, Osipchuk YV, Cahalan MD. Swelling-activated chloride channels in multidrug-sensitive and -resistant cells. J Gen Physiol 1994;**104**:1129–1161.
114. Stobrawa SM, et al. Disruption of ClC-3, a chloride channel expressed on synaptic vesicles, leads to a loss of the hippocampus. Neuron 2001;**29**:185–196.
115. Chien LT, Hartzell HC. Drosophila bestrophin-1 chloride current is dually regulated by calcium and cell volume. J Gen Physiol 2007;**130**:513–524.
116. Yang YD, et al. TMEM16A confers receptor-activated calcium-dependent chloride conductance. Nature 2008;**455**:1210–1215.
117. Deutsch C, Lee SC. Cell volume regulation in lymphocytes. Ren Physiol Biochem 1988;**11**:260–276.
118. Ross PE, Cahalan MD. Ca^{2+} influx pathways mediated by swelling or stores depletion in mouse thymocytes. J Gen Physiol 1995; **106**:415–444.
119. Lee SC, Price M, Prystowsky MB, Deutsch C. Volume response of quiescent and interleukin 2-stimulated T-lymphocytes to hypotonicity. Am J Physiol 1988;**254**: C286–C296.
120. Kerschbaum HH, Cahalan MD. Monovalent permeability, rectification, and ionic block of store-operated calcium channels in Jurkat T lymphocytes. J Gen Physiol 1998;**111**: 521–537.
121. Prakriya M, Lewis RS. Separation and characterization of currents through store-operated CRAC channels and Mg^{2+}-inhibited cation (MIC) channels. J Gen Physiol 2002;**119**:487–507.
122. Hermosura MC, Monteilh-Zoller MK, Scharenberg AM, Penner R, Fleig A. Dissociation of the store-operated calcium current I(CRAC) and the Mg-nucleotide-regulated metal ion current MagNuM. J Physiol 2002;**539**:445–458.
123. Kozak JA, Kerschbaum HH, Cahalan MD. Distinct properties of CRAC and MIC channels in RBL cells. J Gen Physiol 2002;**120**: 221–235.
124. Fomina AF, Fanger CM, Kozak JA, Cahalan MD. Single channel properties and regulated expression of Ca^{2+} release-activated Ca^{2+} (CRAC) channels in human T cells. J Cell Biol 2000;**150**:1435–1444.
125. Jin J, Desai BN, Navarro B, Donovan A, Andrews NC, Clapham DE. Deletion of Trpm7 disrupts embryonic development and thymopoiesis without altering Mg^{2+} homeostasis. Science 2008;**322**:756–760.
126. Kozak JA, Matsushita M, Nairn AC, Cahalan MD. Charge screening by internal pH and polyvalent cations as a mechanism for activation, inhibition, and rundown of TRPM7/MIC channels. J Gen Physiol 2005;**126**:499–514.
127. Tani D, Monteilh-Zoller MK, Fleig A, Penner R. Cell cycle-dependent regulation of store-operated I(CRAC) and Mg^{2+}-nucleotide-regulated MagNuM (TRPM7) currents. Cell Calcium 2007;**41**:249–260.
128. Gwanyanya A, Sipido KR, Vereecke J, Mubagwa K. ATP and PIP2 dependence of the

magnesium-inhibited, TRPM7-like cation channel in cardiac myocytes. Am J Physiol Cell Physiol 2006;**291**:C627–C635.
129. Jiang X, Newell EW, Schlichter LC. Regulation of a TRPM7-like current in rat brain microglia. J Biol Chem 2003;**278**: 42867–42876.
130. Oancea E, Wolfe JT, Clapham DE. Functional TRPM7 channels accumulate at the plasma membrane in response to fluid flow. Circ Res 2006;**98**:245–253.
131. Nadler MJ, et al. LTRPC7 is a Mg.ATP-regulated divalent cation channel required for cell viability. Nature 2001;**411**: 590–595.
132. Runnels LW, Yue L, Clapham DE. TRP-PLIK, a bifunctional protein with kinase and ion channel activities. Science 2001;**291**: 1043–1047.
133. Demeuse P, Penner R, Fleig A. TRPM7 channel is regulated by magnesium nucleotides via its kinase domain. J Gen Physiol 2006;**127**:421–434.
134. Takezawa R, Schmitz C, Demeuse P, Scharenberg AM, Penner R, Fleig A. Receptor-mediated regulation of the TRPM7 channel through its endogenous protein kinase domain. Proc Natl Acad Sci USA 2004;**101**: 6009–6014.
135. Matsushita M, et al. Channel function is dissociated from the intrinsic kinase activity and autophosphorylation of TRPM7/ChaK1. J Biol Chem 2005;**280**:20793–20803.
136. Kozak JA, Cahalan MD. MIC channels are inhibited by internal divalent cations but not ATP. Biophys J 2003;**84**:922–927.
137. Runnels LW, Yue L, Clapham DE. The TRPM7 channel is inactivated by PIP(2) hydrolysis. Nat Cell Biol 2002;**4**:329–336.
138. Suh BC, Hille B. PIP2 is a necessary cofactor for ion channel function: how and why? Annu Rev Biophys 2008;**37**:175–195.
139. Schmitz C, et al. Regulation of vertebrate cellular Mg^{2+} homeostasis by TRPM7. Cell 2003;**114**:191–200.
140. Chubanov V, et al. Disruption of TRPM6/TRPM7 complex formation by a mutation in the TRPM6 gene causes hypomagnesemia with secondary hypocalcemia. Proc Natl Acad Sci USA 2004;**101**: 2894–2899.
141. Sahni J, Scharenberg AM. TRPM7 ion channels are required for sustained phosphoinositide 3-kinase signaling in lymphocytes. Cell Metab 2008;**8**:84–93.
142. Numata T, Shimizu T, Okada Y. TRPM7 is a stretch- and swelling-activated cation channel involved in volume regulation in human epithelial cells. Am J Physiol Cell Physiol 2007;**292**:C460–C467.
143. Brauchi S, Krapivinsky G, Krapivinsky L, Clapham DE. TRPM7 facilitates cholinergic vesicle fusion with the plasma membrane. Proc Natl Acad Sci USA 2008;**105**: 8304–8308.
144. Krapivinsky G, Mochida S, Krapivinsky L, Cibulsky SM, Clapham DE. The TRPM7 ion channel functions in cholinergic synaptic vesicles and affects transmitter release. Neuron 2006;**52**:485–496.
145. Grissmer S, Hanson DC, Natoli EJ, Cahalan MD, Chandy KG. $CD4^-CD8^-$ T cells from mice with collagen arthritis display aberrant expression of type l K^+ channels. J Immunol 1990;**145**:2105–2109.
146. Grissmer S, Cahalan MD, Chandy KG. Abundant expression of type l K^+ channels. A marker for lymphoproliferative diseases? J Immunol 1988;**141**: 1137–1142.
147. Lewis RS, Cahalan MD. Subset-specific expression of potassium channels in developing murine T lymphocytes. Science 1988;**239**:771–775.
148. DeCoursey TE, Chandy KG, Gupta S, Cahalan MD. Two types of potassium channels in murine T lymphocytes. J Gen Physiol 1987;**89**:379–404.
149. Chandy KG, DeCoursey TE, Fischbach M, Talal N, Cahalan MD, Gupta S. Altered K^+ channel expression in abnormal T lymphocytes from mice with the lpr gene mutation. Science 1986;**233**:1197–1200.
150. Chandy KG, Cahalan MD, Grissmer S. Autoimmune diseases linked to abnormal K^+ channel expression in double-negative $CD4^-CD8^-$ T cells. Eur J Immunol 1990; **20**:747–751.
151. Grissmer S, et al. The Shaw-related potassium channel gene, Kv3.1, on human chromosome 11, encodes the type l K^+ channel in T cells. J Biol Chem 1992;**267**:20971–20979.
152. Freedman BD, Fleischmann BK, Punt JA, Gaulton G, Hashimoto Y, Kotlikoff MI. Identification of Kv1.1 expression by murine $CD4^-CD8^-$ thymocytes. A role for voltage-dependent K^+ channels in murine thymocyte development. J Biol Chem 1995;**270**:22406–22411.
153. Liu QH, et al. Modulation of Kv channel expression and function by TCR and costimulatory signals during peripheral $CD4^+$ lymphocyte differentiation. J Exp Med 2002;**196**:897–909.
154. Pottosin II, Bonales-Alatorre E, Valencia-Cruz G, Mendoza-Magana ML, Dobrovinskaya OR. TRESK-like potassium channels in leukemic T cells. Pflugers Arch 2008;**456**:1037–1048.
155. Meuth SG, Bittner S, Meuth P, Simon OJ, Budde T, Wiendl H. TWIK-related acid-sensitive K^+ channel 1 (TASK1) and TASK3 critically influence T lymphocyte effector functions. J Biol Chem 2008;**283**:14559–14570.
156. Grissmer S, Lewis RS, Cahalan MD. Ca^{2+}-activated K^+ channels in human leukemic T cells. J Gen Physiol 1992;**99**:63–84.
157. Jager H, Adelman JP, Grissmer S. SK2 encodes the apamin-sensitive Ca^{2+}-activated K^+ channels in the human leukemic T cell line, Jurkat. FEBS Lett 2000;**469**:196–202.
158. Launay P, Cheng H, Srivatsan S, Penner R, Fleig A, Kinet JP. TRPM4 regulates calcium oscillations after T cell activation. Science 2004;**306**:1374–1377.
159. Beck A, Kolisek M, Bagley LA, Fleig A, Penner R. Nicotinic acid adenine dinucleotide phosphate and cyclic ADP-ribose regulate TRPM2 channels in T lymphocytes. FASEB J 2006;**20**:962–964.
160. Su Z, Guo X, Barker DS, Shoemaker RL, Marchase RB, Blalock JE. A store-operated nonselective cation channel in human lymphocytes. Cell Mol Neurobiol 2005;**25**:625–647.
161. Sano Y, et al. Immunocyte Ca^{2+} influx system mediated by LTRPC2. Science 2001; **293**:1327–1330.
162. Gasser A, et al. Activation of T cell calcium influx by the second messenger ADP-ribose. J Biol Chem 2006;**281**:2489–2496.
163. Schwarz EC, et al. TRP channels in lymphocytes. Handb Exp Pharmacol 2007;**179**:445–456.
164. Inada H, Iida T, Tominaga M. Different expression patterns of TRP genes in murine B and T lymphocytes. Biochem Biophys Res Commun 2006;**350**:762–767.
165. Hess SD, Oortgiesen M, Cahalan MD. Calcium oscillations in human T and natural killer cells depend upon membrane potential and calcium influx. J Immunol 1993;**150**:2620–2633.
166. Leonard RJ, Garcia ML, Slaughter RS, Reuben JP. Selective blockers of voltage-gated K^+ channels depolarize human T lymphocytes: mechanism of the antiproliferative effect of charybdotoxin. Proc Natl Acad Sci USA 1992;**89**:10094–10098.
167. Deutsch C, Price M. Role of extracellular Na and K in lymphocyte activation. J Cell Physiol 1982;**113**:73–79.
168. Badou A, et al. Critical role for the beta regulatory subunits of Cav channels in T lymphocyte function. Proc Natl Acad Sci USA 2006;**103**:15529–15534.
169. Badou A, et al. Requirement of voltage-gated calcium channel beta4 subunit for T lymphocyte functions. Science 2005;**307**:117–121.
170. Kotturi MF, Hunt SV, Jefferies WA. Roles of CRAC and Cav-like channels in T cells: more than one gatekeeper? Trends Pharmacol Sci 2006;**27**:360–367.
171. Kotturi MF, Carlow DA, Lee JC, Ziltener HJ, Jefferies WA. Identification and functional characterization of voltage-dependent cal-

cium channels in T lymphocytes. J Biol Chem 2003;**278**:46949–46960.
172. Kotturi MF, Jefferies WA. Molecular characterization of L-type calcium channel splice variants expressed in human T lymphocytes. Mol Immunol 2005;**42**:1461–1474.
173. Gomes B, et al. Lymphocyte calcium signaling involves dihydropyridine-sensitive L-type calcium channels: facts and controversies. Crit Rev Immunol 2004;**24**:425–447.
174. Grafton G, Stokes L, Toellner KM, Gordon J. A non-voltage-gated calcium channel with L-type characteristics activated by B cell receptor ligation. Biochem Pharmacol 2003;**66**:2001–2009.
175. Stokes L, Gordon J, Grafton G. Non-voltage-gated L-type Ca^{2+} channels in human T cells: pharmacology and molecular characterization of the major alpha pore-forming and auxiliary beta-subunits. J Biol Chem 2004;**279**:19566–19573.
176. Feske S, Prakriya M, Rao A, Lewis RS. A severe defect in CRAC Ca^{2+} channel activation and altered K^+ channel gating in T cells from immunodeficient patients. J Exp Med 2005;**202**:651–662.
177. Gwack Y, et al. Hair loss and defective T and B cell function in mice lacking ORAI1. Mol Cell Biol 2008;**28**:5209–5222.
178. Poenie M, Tsien RY, Schmitt-Verhulst AM. Sequential activation and lethal hit measured by $[Ca^{2+}]_i$ in individual cytolytic T cells and targets. EMBO J 1987;**6**:2223–2232.
179. Tsien RY, Rink TJ, Poenie M. Measurement of cytosolic free Ca^{2+} in individual small cells using fluorescence microscopy with dual excitation wavelengths. Cell Calcium 1985;**6**:145–157.
180. Donnadieu E, Bismuth G, Trautmann A. Calcium fluxes in T lymphocytes. J Biol Chem 1992;**267**:25864–25872.
181. Fanger CM, et al. Calcium-activated potassium channels sustain calcium signaling in T lymphocytes. Selective blockers and manipulated channel expression levels. J Biol Chem 2001;**276**:12249–12256.
182. Donnadieu E, Bismuth G, Trautmann A. Antigen recognition by helper T cells elicits a sequence of distinct changes of their shape and intracellular calcium. Curr Biol 1994;**4**:584–595.
183. Donnadieu E, Cefai D, Tan YP, Paresys G, Bismuth G, Trautmann A. Imaging early steps of human T cell activation by antigen-presenting cells. J Immunol 1992;**148**:2643–2653.
184. Negulescu PA, Krasieva TB, Khan A, Kerschbaum HH, Cahalan MD. Polarity of T cell shape, motility, and sensitivity to antigen. Immunity 1996;**4**:421–430.
185. Bhakta NR, Oh DY, Lewis RS. Calcium oscillations regulate thymocyte motility during positive selection in the three-dimensional thymic environment. Nat Immunol 2005;**6**:143–151.
186. Wei SH, Safrina O, Yu Y, Garrod KR, Cahalan MD, Parker I. Ca^{2+} signals in $CD4^+$ T cells during early contacts with antigen-bearing dendritic cells in lymph node. J Immunol 2007;**179**:1586–1594.
187. Skokos D, et al. Peptide–MHC potency governs dynamic interactions between T cells and dendritic cells in lymph nodes. Nat Immunol 2007;**8**:835–844.
188. Miller MJ, Hejazi AS, Wei SH, Cahalan MD, Parker I. T cell repertoire scanning is promoted by dynamic dendritic cell behavior and random T cell motility in the lymph node. Proc Natl Acad Sci USA 2004;**101**:998–1003.
189. Wei X, Tromberg BJ, Cahalan MD. Mapping the sensitivity of T cells with an optical trap: polarity and minimal number of receptors for Ca^{2+} signaling. Proc Natl Acad Sci USA 1999;**96**:8471–8476.
190. Dustin ML. Hunter to gatherer and back: immunological synapses and kinapses as variations on the theme of amoeboid locomotion. Annu Rev Cell Dev Biol 2008;**24**:577–596.
191. Cahalan MD, Parker I. Choreography of cell motility and interaction dynamics imaged by two-photon microscopy in lymphoid organs. Annu Rev Immunol 2008;**26**:585–626.
192. Negulescu PA, Shastri N, Cahalan MD. Intracellular calcium dependence of gene expression in single T lymphocytes. Proc Natl Acad Sci USA 1994;**91**:2873–2877.
193. Dolmetsch RE, Lewis RS, Goodnow CC, Healy JI. Differential activation of transcription factors induced by Ca^{2+} response amplitude and duration. Nature 1997;**386**:855–858.
194. Dolmetsch RE, Xu K, Lewis RS. Calcium oscillations increase the efficiency and specificity of gene expression. Nature 1998;**392**:933–936.
195. Feske S, Giltnane J, Dolmetsch R, Staudt LM, Rao A. Gene regulation mediated by calcium signals in T lymphocytes. Nat Immunol 2001;**2**:316–324.
196. Panyi G, et al. Kv1.3 potassium channels are localized in the immunological synapse formed between cytotoxic and target cells. Proc Natl Acad Sci USA 2004;**101**:1285–1290.
197. Nicolaou SA, Neumeier L, Peng Y, Devor DC, Conforti L. The Ca^{2+}-activated K^+ channel KCa3.1 compartmentalizes in the immunological synapse of human T lymphocytes. Am J Physiol Cell Physiol 2007;**292**:C1431–C1439.
198. Nicolaou SA, Neumeier L, Peng Y, Devor D, Conforti L. The Ca^{2+}-activated K channel KCa3.1 compartmentalizes in the immunological synapse of human T lymphocytes. Am J Physiol Cell Physiol 2006;**292**:C1431–C1439.
199. Panyi G, et al. Colocalization and nonrandom distribution of Kv1.3 potassium channels and CD3 molecules in the plasma membrane of human T lymphocytes. Proc Natl Acad Sci USA 2003;**100**:2592–2597.
200. Rus H, et al. The voltage-gated potassium channel Kv1.3 is highly expressed on inflammatory infiltrates in multiple sclerosis brain. Proc Natl Acad Sci USA 2005;**102**:11094–11099.
201. Krummel MF, Sjaastad MD, Wulfing C, Davis MM. Differential clustering of CD4 and CD3zeta during T cell recognition. Science 2000;**289**:1349–1352.
202. Zweifach A, Lewis RS. Slow calcium-dependent inactivation of depletion-activated calcium current. Store-dependent and -independent mechanisms. J Biol Chem 1995;**270**:14445–14451.
203. Zweifach A, Lewis RS. Rapid inactivation of depletion-activated calcium current (ICRAC) due to local calcium feedback. J Gen Physiol 1995;**105**:209–226.
204. Malli R, Naghdi S, Romanin C, Graier WF. Cytosolic Ca^{2+} prevents the subplasmalemmal clustering of STIM1: an intrinsic mechanism to avoid Ca^{2+} overload. J Cell Sci 2008;**121**:3133–3139.
205. Hoth M, Button DC, Lewis RS. Mitochondrial control of calcium-channel gating: a mechanism for sustained signaling and transcriptional activation in T lymphocytes. Proc Natl Acad Sci USA 2000;**97**:10607–10612.
206. Hoth M, Fanger CM, Lewis RS. Mitochondrial regulation of store-operated calcium signaling in T lymphocytes. J Cell Biol 1997;**137**:633–648.
207. Quintana A, Kummerow C, Junker C, Becherer U, Hoth M. Morphological changes of T cells following formation of the immunological synapse modulate intracellular calcium signals. Cell Calcium 2009;**45**:109–122.
208. Quintana A, et al. T cell activation requires mitochondrial translocation to the immunological synapse. Proc Natl Acad Sci USA 2007;**104**:14418–14423.
209. Brossard C, et al. Multifocal structure of the T cell–dendritic cell synapse. Eur J Immunol 2005;**35**:1741–1753.
210. McCann FE, et al. The size of the synaptic cleft and distinct distributions of filamentous actin, ezrin, CD43, and CD45 at activating and inhibitory human NK cell immune synapses. J Immunol 2003;**170**:2862–2870.
211. Burroughs NJ, Wulfing C. Differential segregation in a cell-cell contact interface: the dynamics of the immunological synapse. Biophys J 2002;**83**:1784–1796.

212. Wild MK, et al. Dependence of T cell antigen recognition on the dimensions of an accessory receptor-ligand complex. J Exp Med 1999;**190**:31–41.
213. Katz B, Miledi R. An endplate potential due to potassium released by the motor nerve impulse. Proc R Soc Lond B Biol Sci 1982;**216**:497–507.
214. Montes M, McIlroy D, Hosmalin A, Trautmann A. Calcium responses elicited in human T cells and dendritic cells by cell-cell interaction and soluble ligands. Int Immunol 1999;**11**:561–568.
215. Vukcevic M, Spagnoli GC, Iezzi G, Zorzato F, Treves S. Ryanodine receptor activation by Ca v 1.2 is involved in dendritic cell major histocompatibility complex class II surface expression. J Biol Chem 2008;**283**:34913–34922.
216. Hsu S, et al. Fundamental Ca^{2+} signaling mechanisms in mouse dendritic cells: CRAC is the major Ca^{2+} entry pathway. J Immunol 2001;**166**:6126–6133.
217. Joung I, et al. Modification of Ser59 in the unique N-terminal region of tyrosine kinase p56lck regulates specificity of its Src homology 2 domain. Proc Natl Acad Sci USA 1995;**92**:5778–5782.
218. Park I, Chung J, Walsh CT, Yun Y, Strominger JL, Shin J. Phosphotyrosine-independent binding of a 62-kDa protein to the src homology 2 (SH2) domain of p56lck and its regulation by phosphorylation of Ser-59 in the lck unique N-terminal region. Proc Natl Acad Sci USA 1995;**92**:12338–12342.
219. Vadlamudi RK, Joung I, Strominger JL, Shin J. p62, a phosphotyrosine-independent ligand of the SH2 domain of p56lck, belongs to a new class of ubiquitin-binding proteins. J Biol Chem 1996;**271**:20235–20237.
220. Diradourian C, Le May C, Cauzac M, Girard J, Burnol AF, Pegorier JP. Involvement of ZIP/p62 in the regulation of PPARalpha transcriptional activity by p38-MAPK. Biochim Biophys Acta 2008;**1781**:239–244.
221. Kim JY, Ozato K. The sequestosome 1/p62 attenuates cytokine gene expression in activated macrophages by inhibiting IFN regulatory factor 8 and TNF receptor-associated factor 6/NF-kappaB activity. J Immunol 2009;**182**:2131–2140.
222. Gong J, Xu J, Bezanilla M, van Huizen R, Derin R, Li M. Differential stimulation of PKC phosphorylation of potassium channels by ZIP1 and ZIP2. Science 1999;**285**:1565–1569.
223. Real E, Faure S, Donnadieu E, Delon J. Cutting edge: Atypical PKCs regulate T lymphocyte polarity and scanning behavior. J Immunol 2007;**179**:5649–5652.
224. Robbins JR, et al. Hypoxia modulates early events in T cell receptor-mediated activation in human T lymphocytes via Kv1.3 channels. J Physiol 2005;**564**:131–143.
225. Szigligeti P, et al. Signalling during hypoxia in human T lymphocytes – critical role of the src protein tyrosine kinase p56Lck in the O2 sensitivity of Kv1.3 channels. J Physiol 2006;**573**:357–370.
226. Pursiheimo JP, Rantanen K, Heikkinen PT, Johansen T, Jaakkola PM. Hypoxia-activated autophagy accelerates degradation of SQSTM1/p62. Oncogene 2009;**28**:334–344.
227. Gulbis JM, Mann S, MacKinnon R. Structure of a voltage-dependent K^+ channel beta subunit. Cell 1999;**97**:943–952.
228. Tipparaju SM, Barski OA, Srivastava S, Bhatnagar A. Catalytic mechanism and substrate specificity of the beta-subunit of the voltage-gated potassium channel. Biochemistry 2008;**47**:8840–8854.
229. Campomanes CR, et al. Kv beta subunit oxidoreductase activity and Kv1 potassium channel trafficking. J Biol Chem 2002;**277**:8298–8305.
230. Hanada T, Lin L, Chandy KG, Oh SS, Chishti AH. Human homologue of the Drosophila discs large tumor suppressor binds to p56lck tyrosine kinase and Shaker type Kv1.3 potassium channel in T lymphocytes. J Biol Chem 1997;**272**:26899–26904.
231. Hanada N, et al. NE-dlg, a mammalian homolog of Drosophila dlg tumor suppressor, induces growth suppression and impairment of cell adhesion: possible involvement of down-regulation of beta-catenin by NE-dlg expression. Int J Cancer 2000;**86**:480–488.
232. Levite M, et al. Extracellular K^+ and opening of voltage-gated potassium channels activate T cell integrin function: physical and functional association between Kv1.3 channels and beta1 integrins. J Exp Med 2000;**191**:1167–1176.
233. Gulbins E, Szabo I, Baltzer K, Lang F. Ceramide-induced inhibition of T lymphocyte voltage-gated potassium channel is mediated by tyrosine kinases. Proc Natl Acad Sci USA 1997;**94**:7661–7666.
234. Szabo I, et al. Tyrosine phosphorylation-dependent suppression of a voltage-gated K^+ channel in T lymphocytes upon Fas stimulation. J Biol Chem 1996;**271**:20465–20469.
235. Fadool DA. Tyrosine phosphorylation downregulates a potassium current in rat olfactory bulb neurons and a cloned Kv1.3 channel. Ann N Y Acad Sci 1998;**855**:529–532.
236. Holmes TC, Fadool DA, Levitan IB. Tyrosine phosphorylation of the Kv1.3 potassium channel. J Neurosci 1996;**16**:1581–1590.
237. Fournier HN, et al. Integrin cytoplasmic domain-associated protein 1alpha (ICAP-1alpha) interacts directly with the metastasis suppressor nm23-H2, and both proteins are targeted to newly formed cell adhesion sites upon integrin engagement. J Biol Chem 2002;**277**:20895–20902.
238. Gupta S. Autologous mixed-lymphocyte reaction in man. XVII. In vitro effect of ion channel-blocking agents on the autologous mixed-lymphocyte response. Cell Immunol 1987;**104**:290–295.
239. Price M, Lee SC, Deutsch C. Charybdotoxin inhibits proliferation and interleukin 2 production in human peripheral blood lymphocytes. Proc Natl Acad Sci USA 1989;**86**:10171–10175.
240. Sabath DE, Monos DS, Lee SC, Deutsch C, Prystowsky MB. Cloned T-cell proliferation and synthesis of specific proteins are inhibited by quinine. Proc Natl Acad Sci USA 1986;**83**:4739–4743.
241. Hu L, Pennington M, Jiang Q, Whartenby KA, Calabresi PA. Characterization of the functional properties of the voltage-gated potassium channel Kv1.3 in human $CD4^+$ T lymphocytes. J Immunol 2007;**179**:4563–4570.
242. Lin CS, et al. Voltage-gated potassium channels regulate calcium-dependent pathways involved in human T lymphocyte activation. J Exp Med 1993;**177**:637–645.
243. Verheugen JA, Le Deist F, Devignot V, Korn H. Enhancement of calcium signaling and proliferation responses in activated human T lymphocytes. Inhibitory effects of K^+ channel block by charybdotoxin depend on the T cell activation state. Cell Calcium 1997;**21**:1–17.
244. Ren YR, et al. Clofazimine inhibits human Kv1.3 potassium channel by perturbing calcium oscillation in T lymphocytes. PLoS ONE 2008;**3**:e4009.
245. Mello de Queiroz F, Ponte CG, Bonomo A, Vianna-Jorge R, Suarez-Kurtz G. Study of membrane potential in T lymphocytes subpopulations using flow cytometry. BMC Immunol 2008;**9**:63.
246. Mestas J, Hughes CC. Of mice and not men: differences between mouse and human immunology. J Immunol 2004;**172**:2731–2738.
247. Beeton C, Chandy KG. Potassium channels, memory T cells, and multiple sclerosis. Neuroscientist 2005;**11**:550–562.
248. Wulff H, et al. The voltage-gated Kv1.3 K^+ channel in effector memory T cells as new target for MS. J Clin Invest 2003;**111**:1703–1713.
249. DeCoursey TE, Chandy KG, Gupta S, Cahalan MD. Mitogen induction of ion channels in murine T lymphocytes. J Gen Physiol 1987;**89**:405–420.

250. Deutsch C, Krause D, Lee SC. Voltage-gated potassium conductance in human T lymphocytes stimulated with phorbol ester. J Physiol 1986;**372**: 405–423.
251. Lewis RS, Cahalan MD. The plasticity of ion channels: parallels between the nervous and immune systems. Trends Neurosci 1988;**11**:214–218.
252. Reich EP, et al. Blocking ion channel KCNN4 alleviates the symptoms of experimental autoimmune encephalomyelitis in mice. Eur J Immunol 2005;**35**: 1027–1036.
253. Fanger CM, Neben AL, Cahalan MD. Differential Ca^{2+} influx, KCa channel activity, and Ca^{2+} clearance distinguish Th1 and Th2 lymphocytes. J Immunol 2000;**164**: 1153–1160.
254. Sloan-Lancaster J, Steinberg TH, Allen PM. Selective loss of the calcium ion signaling pathway in T cells maturing toward a T helper 2 phenotype. J Immunol 1997;**159**:1160–1168.
255. Weber KS, Miller MJ, Allen PM. Th17 cells exhibit a distinct calcium profile from Th1 and Th2 cells and have Th1-like motility and NF-AT nuclear localization. J Immunol 2008;**180**:1442–1450.
256. Wulff H, Knaus HG, Pennington M, Chandy KG. K^+ channel expression during B cell differentiation: implications for immunomodulation and autoimmunity. J Immunol 2004;**173**:776–786.
257. Partiseti M, Choquet D, Diu A, Korn H. Differential regulation of voltage- and calcium-activated potassium channels in human B lymphocytes. J Immunol 1992;**148**: 3361–3368.
258. Partiseti M, Korn H, Choquet D. Pattern of potassium channel expression in proliferating B lymphocytes depends upon the mode of activation. J Immunol 1993;**151**:2462–2470.
259. Amigorena S, Choquet D, Teillaud JL, Korn H, Fridman WH. Ion channel blockers inhibit B cell activation at a precise stage of the G1 phase of the cell cycle. Possible involvement of K^+ channels. J Immunol 1990;**144**:2038–2045.
260. Garrod KR, Wei SH, Parker I, Cahalan MD. Natural killer cells actively patrol peripheral lymph nodes forming stable conjugates to eliminate MHC-mismatched targets. Proc Natl Acad Sci USA 2007;**104**: 12081–12086.
261. Schlichter L, Sidell N, Hagiwara S. K channels are expressed early in human T-cell development. Proc Natl Acad Sci USA 1986;**83**:5625–5629.
262. Sidell N, Schlichter LC, Wright SC, Hagiwara S, Golub SH. Potassium channels in human NK cells are involved in discrete stages of the killing process. J Immunol 1986;**137**:1650–1658.
263. Lee SC, Sabath DE, Deutsch C, Prystowsky MB. Increased voltage-gated potassium conductance during interleukin 2-stimulated proliferation of a mouse helper T lymphocyte clone. J Cell Biol 1986;**102**:1200–1208.
264. Bousso P, Bhakta NR, Lewis RS, Robey E. Dynamics of thymocyte-stromal cell interactions visualized by two-photon microscopy. Science 2002;**296**:1876–1880.
265. Cahalan MD, Parker I, Wei SH, Miller MJ. Two-photon tissue imaging: seeing the immune system in a fresh light. Nat Rev Immunol 2002;**2**:872–880.
266. Miller MJ, Wei SH, Cahalan MD, Parker I. Autonomous T cell trafficking examined in vivo with intravital two-photon microscopy. Proc Natl Acad Sci USA 2003;**100**:2604–2609.
267. Mempel TR, Henrickson SE, Von Andrian UH. T-cell priming by dendritic cells in lymph nodes occurs in three distinct phases. Nature 2004;**427**:154–159.
268. Miller MJ, Safrina O, Parker I, Cahalan MD. Imaging the single cell dynamics of $CD4^+$ T cell activation by dendritic cells in lymph nodes. J Exp Med 2004;**200**:847–856.
269. Okada T, et al. Antigen-engaged B cells undergo chemotaxis toward the T zone and form motile conjugates with helper T cells. PLoS Biol 2005;**3**:1047–1061.
270. Lewis RS. The molecular choreography of a store-operated calcium channel. Nature 2007;**446**:284–287.
271. Cahalan MD, Zhang SL, Yeromin AV, Ohlsen K, Roos J, Stauderman KA. Molecular basis of the CRAC channel. Cell Calcium 2007;**42**:133–144.
272. Feske S. Calcium signalling in lymphocyte activation and disease. Nat Rev Immunol 2007;**7**:690–702.
273. Mandala S, et al. Alteration of lymphocyte trafficking by sphingosine-1-phosphate receptor agonists. Science 2002;**296**:346–349.
274. Sanna MG, et al. Enhancement of capillary leakage and restoration of lymphocyte egress by a chiral S1P(1) antagonist in vivo. Nat Chem Biol 2006;**2**:434–441.
275. Wei SH, et al. Sphingosine 1-phosphate type 1 receptor agonism inhibits transendothelial migration of medullary T cells to lymphatic sinuses. Nat Immunol 2005;**6**:1228–1235.
276. Matheu MP, et al. Imaging of effector memory T cells during a delayed-type hypersensitivity reaction and suppression by Kv1.3 channel block. Immunity 2008;**29**:602–614.
277. Kawakami N, Nagerl UV, Odoardi F, Bonhoeffer T, Wekerle H, Flugel A. Live imaging of effector cell trafficking and autoantigen recognition within the unfolding autoimmune encephalomyelitis lesion. J Exp Med 2005;**201**:1805–1814.
278. Wulff H, Beeton C, Chandy KG. Potassium channels as therapeutic targets for autoimmune disorders. Curr Opin Drug Discov Devel 2003;**6**:640–647.
279. Beeton C, et al. Targeting effector memory T cells with a selective peptide inhibitor of Kv1.3 channels for therapy of autoimmune diseases. Mol Pharmacol 2005;**67**:1369–1381.
280. Azam P, Sankaranarayanan A, Homerick D, Griffey S, Wulff H. Targeting effector memory T cells with the small molecule Kv1.3 blocker PAP-1 suppresses allergic contact dermatitis. J Invest Dermatol 2007;**127**:1419–1429.
281. Beeton C, et al. Selective blocking of voltage-gated K^+ channels improves experimental autoimmune encephalomyelitis and inhibits T cell activation. J Immunol 2001;**166**:936–944.
282. Beeton C, et al. The D-diastereomer of ShK toxin selectively blocks voltage-gated K^+ channels and inhibits T lymphocyte proliferation. J Biol Chem 2008;**283**: 988–997.
283. Valverde P, Kawai T, Taubman MA. Selective blockade of voltage-gated potassium channels reduces inflammatory bone resorption in experimental periodontal disease. J Bone Miner Res 2004;**19**:155–164.
284. Valverde P, Kawai T, Taubman MA. Potassium channel-blockers as therapeutic agents to interfere with bone resorption of periodontal disease. J Dent Res 2005;**84**:488–499.
285. Koo GC, et al. Correolide and derivatives are novel immunosuppressants blocking the lymphocyte Kv1.3 potassium channels. Cell Immunol 1999;**197**:99–107.
286. Koo GC, et al. Blockade of the voltage-gated potassium channel Kv1.3 inhibits immune responses in vivo. J Immunol 1997;**158**:5120–5128.
287. Craythorn JM, Swartz M, Creel DJ. Clofazimine-induced bull's-eye retinopathy. Retina 1986;**6**:50–52.
288. Mathew BS, Pulimood AB, Prasanna CG, Ramakrishna BS, Chandy SJ. Clofazimine induced enteropathy – a case highlighting the importance of drug induced disease in differential diagnosis. Trop Gastroenterol 2006;**27**:87–88.
289. McDougall AC, Horsfall WR, Hede JE, Chaplin AJ. Splenic infarction and tissue accumulation of crystals associated with the use of clofazimine (Lamprene; B663) in the treatment of pyoderma gangrenosum. Br J Dermatol 1980;**102**:227–230.
290. Parizhskaya M, Youssef NN, Di Lorenzo C, Goyal RK. Clofazimine enteropathy in a

pediatric bone marrow transplant recipient. J Pediatr 2001;**138**:574–576.
291. Pereira LE, Villinger F, Wulff H, Sankaranarayanan A, Raman G, Ansari AA. Pharmacokinetics, toxicity, and functional studies of the selective kv1.3 channel blocker 5-(4-phenoxybutoxy) psoralen in rhesus macaques. Exp Biol Med (Maywood) 2007;**232**: 1338–1354.
292. Stathopulos PB, Zheng L, Li GY, Plevin MJ, Ikura M. Structural and mechanistic insights into STIM1-mediated initiation of store-operated calcium entry. Cell 2008;**135**: 110–122.
293. Yamaguchi H, Matsushita M, Nairn AC, Kuriyan J. Crystal structure of the atypical protein kinase domain of a TRP channel with phosphotransferase activity. Mol Cell 2001;**7**:1047–1057.